Clim. Past, 7, 91–114, 2011
www.clim-past.net/7/91/2011/
doi:10.5194/cp-7-91-2011

Climate of the Past

A comparison of climate simulations for the last glacial maximum with three different versions of the ECHAM model and implications for summer-green tree refugia

K. Arpe[1,2], **S. A. G. Leroy**[1], **and U. Mikolajewicz**[2]

[1]Institute for the Environment, Brunel University, West London, UK
[2]Max Planck Institute for Meteorology, Hamburg, Germany

Received: 16 March 2010 – Published in Clim. Past Discuss.: 20 April 2010
Revised: 6 January 2011 – Accepted: 16 January 2011 – Published: 22 February 2011

Abstract. Model simulations of the last glacial maximum (21 ± 2 ka) with the ECHAM3 T42 atmosphere-only, ECHAM5-MPIOM T31 atmosphere-ocean coupled and ECHAM5 T106 atmosphere-only models are compared. The topography, land-sea mask and glacier distribution for the ECHAM5 simulations were taken from the Paleoclimate Modelling Intercomparison Project Phase II (PMIP2) data set while for ECHAM3 they were taken from PMIP1. The ECHAM5-MPIOM T31 model produced its own sea surface temperatures (SST) while the ECHAM5 T106 simulations were forced at the boundaries by this coupled model SSTs corrected from their present-day biases and the ECHAM3 T42 model was forced with prescribed SSTs provided by Climate/Long-Range Investigation, Mapping, and Prediction project (CLIMAP).

The SSTs in the ECHAM5-MPIOM simulation for the last glacial maximum (LGM) were much warmer in the northern Atlantic than those suggested by CLIMAP or Overview of Glacial Atlantic Ocean Mapping (GLAMAP) while the SSTs were cooler everywhere else. This had a clear effect on the temperatures over Europe, warmer for winters in western Europe and cooler for eastern Europe than the simulation with CLIMAP SSTs.

Considerable differences in the general circulation patterns were found in the different simulations. A ridge over western Europe for the present climate during winter in the 500 hPa height field remains in both ECHAM5 simulations for the LGM, more so in the T106 version, while the ECHAM3 CLIMAP-SST simulation provided a trough which is consistent with cooler temperatures over western Europe. The zonal wind between 30° W and 10° E shows a southward shift of the polar and subtropical jets in the simulations for the LGM, least obvious in the ECHAM5 T31 one, and an extremely strong polar jet for the ECHAM3 CLIMAP-SST run. The latter can probably be assigned to the much stronger north-south gradient in the CLIMAP SSTs. The southward shift of the polar jet during the LGM is supported by palaeo-data.

Cyclone tracks in winter represented by high precipitation are characterised over Europe for the present by a main branch from the British Isles to Norway and a secondary branch towards the Mediterranean Sea, observed and simulated. For the LGM the different models show very different solutions: the ECHAM3 CLIMAP-SST simulation shows just one track going eastward from the British Isles into central Europe, while the ECHAM5 T106 simulation still has two branches but during the LGM the main one goes to the Mediterranean Sea, with enhanced precipitation in the Levant. This agrees with an observed high stand of the Dead Sea during the LGM. For summer the ECHAM5 T106 simulation provides much more precipitation for the present over Europe than the other simulations, thus agreeing with estimates by the Global Precipitation Climatology Project (GPCP). Also during the LGM this model makes Europe less arid than the other simulations.

In many respects the ECHAM5 T106 simulation for the present is more realistic than the ECHAM5 T31 coupled simulation and the older ECHAM3 T42 simulation, when comparing them with the European Centre for Medium-Range Weather Forecasts (ECMWF) reanalysis or the GPCP precipitation data. For validating the model data for the LGM, pollen, wood and charcoal analyses were compared with possible summer-green tree growth from model estimates

Correspondence to: S. A. G. Leroy
(suzanne.leroy@brunel.ac.uk)

Published by Copernicus Publications on behalf of the European Geosciences Union.

using summer precipitation, minimum winter temperatures and growing degree days (above 5 °C). The ECHAM5 T106 simulation suggests for more sites with findings of palaeo-data, likely tree growth during the LGM than the other simulations, especially over western Europe. The clear message especially from the ECHAM5 T106 simulation is that warm-loving summer-green trees could have survived mainly in Spain but also in Greece in agreement with findings of pollen or charcoal. Southern Italy is also suggested but this could not be validated because of absence of palaeo-data.

Previous climate simulations of the LGM have suggested less cold and more humid climate than that reconstructed from pollen findings. Our model results do agree more or less with those of other models but we do not find a contradiction with palaeo-data because we use the pollen data directly without an intermediate reconstruction of temperatures and precipitation from the pollen spectra.

1 Introduction

In the light of climatic change investigations, the climate during the Last Glacial Maximum (LGM) is of special interest because of its extreme conditions. Plant and animal remains from the LGM have been widely used to reconstruct the climate of the LGM (e.g. CLIMAP, 1981; Grosswald, 1980; Tarasov et al., 1999). It has generally been assumed that the climate in Europe was much more arid and colder than the present climate. Climate simulations of the LGM suggest, however, a less cold and more humid climate than that from reconstruction from pollen findings (e.g. Svenning et al., 2008). Recently this picture is changing owing to an international modelling effort and improved temperature reconstruction. These new estimates of precipitation and temperature from pollen findings brought a better agreement to climate based on model simulations of the LGM carried out, e.g. in the framework of the Paleoclimate Modelling Intercomparison Project Phase II (PMIP2) by Kageyama et al. (2007) or Braconnot et al. (2007). For instance, less arid and less cold conditions were reconstructed from palaeo-data by taking into account the impact of lower CO_2 on pollen production during the LGM. Using the reconstruction of Wu et al. (2007) leads to a better resemblance with model results according to Ramstein et al. (2007).

In addition to the intrinsic importance of reconstructing the general circulation during the LGM it is essential to establish the potential location of tree refugia, as both animals and humans depended on them for their survival. Leroy and Arpe (2007), referred to below as LA2007, investigated possible summer-green tree refugia during the LGM using the simulated climate data for the present and the LGM. The simulations had been carried out with the ECHAM3 (ECHAM consists out of 2 groups of letters: EC for ECMWF, the institute from where the model originated, and HAM for Hamburg, where the modifications for the present climate model have been made) (Roeckner et al., 1992) atmospheric model which had a spectral resolution of T42 (corresponds to approx. 2.8° horizontal resolution) and 19 levels in the vertical and was forced with the Sea Surface Temperature (SST) provided by the Climate/Long-Range Investigation, Mapping, and Prediction project (CLIMAP, 1981). Lorenz et al. (1996) described the set up for these simulations. LA2007 highlighted as possible refugia for summer-green trees, small areas within the three southern peninsulas of Europe (Spain, Italy and Greece). Further, areas that have remained poorly known were then proposed as refugia, including the Sakarya-Kerempe region in northern Turkey, the east coast of the Black Sea and the area south of the Caspian Sea. A similar investigation was carried out by Cheddadi et al. (2006) using probably the same ECHAM data as well as data from another model and a similar down-scaling for one evergreen tree species, *Pinus sylvestris*. They found a simulated distribution of *P. sylvestris* during the LGM which is coherent with the observed fossil data, which showed a patchy distribution of the refugia between 40 and 50° N, i.e. a belt further north of that for summer-green trees dealt with by LA2007. Model development, however, is an on-going process and the resolution was quite coarse for this type of investigation; this can be an issue for sites of observed tree refugia in quite topographically structured areas.

To improve on past studies it was decided to carry out simulations with a more modern model and with a higher spatial resolution. Therefore a new simulation with a high resolution (T106) version of the ECHAM5 model has been carried out. The results from this new simulation are compared in this paper with the results from already existing simulations with the ECHAM model. As our vegetation data are from Europe and western Asia, our analysis focuses on the climate of Europe, eastwards up to the Caspian Sea. We do not only investigate possible refugia of summer-green trees but also discuss some basic quantities which should improve the understanding of the performance of the model. The method used here required also simulations for the present climate. These are also investigated in detail to understand the performance of the models, as it is only for the present climate that a large amount of data for validation is available. The study is further improved in relation to LA2007 by the inclusion of more sites with observed summer-green tree growth during the LGM, partly from new studies and partly from further literature research.

In Sect. 2 of this paper the model simulations and their setup are described. In Sect. 3 the climates obtained in the different model simulations are compared and differences between them discussed. In Sect. 4 limits of the distribution of warm and cold-loving trees are derived from these climate simulations using various criteria. The model derived estimates of potential refugia are compared to findings from pollen, charcoal and fossil wood records which have been selected on criteria of strength of the signal and quality of

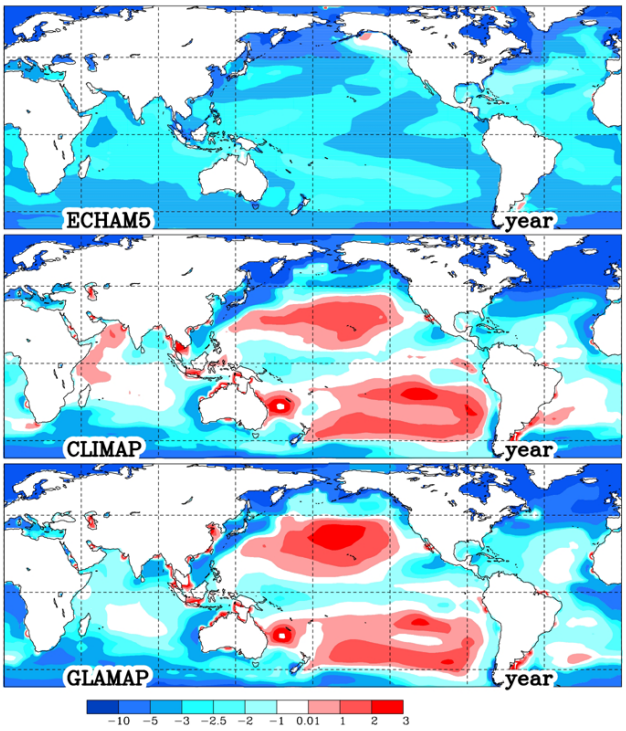

Fig. 1. Annual mean SST differences between the LGM and the present (NOW). Contours at −10, −5, −3, −2.5, −2, −1, −0.01, 1, 2, 3 °C. Data from the models used here are surface temperatures which over sea ice can become very low.

the chronology. For the latter a set of criteria was defined in order to include or exclude sites to be considered by our analysis. This is discussed in Sect. 4.

2 Description of the simulations

The three LGM simulations available at the Max-Planck Institute (MPI) for Meteorology in Hamburg represent different generations of climatic models and different resolutions. The simulations have been performed in three different resolutions (T106, T42, and T31) with the old model version ECHAM3 and the actual model version ECHAM5. The names of the experiments are a combination of the resolution and the model version (T??EH?). Table 1 gives an overview of the naming and conditions for the three sets of simulations.

In the old experiments with ECHAM3 (henceforth T42EH3) the SST anomalies including the sea-ice cover were provided by CLIMAP (1981) for the globe but from an inspection (Fig. 1) it seems to be reconstructed only for the northern hemisphere as the SSTs for the LGM differed only slightly from those for the present for the rest of the world, which is hardly realistic. Also, PMIP2 simulations (Braconnot et al., 2007) contained this inconsistency that was confirmed by new tropical SSTs reconstructions from the MARGO project (Kucera et al., 2005). Therefore the

Table 1. SST × resolution atmospheric model.

name	SST	resolution	atmospheric model
T42EH3	CLIMAP anomalies	T42L19–2.8125° 19 levels	ECHAM3
T31EH5	coupled	T31L19–3.75° 19 levels	ECHAM5
T106EH5	T31EH5 anomalies	T106L39–1.125° 39 levels	ECHAM5

coupled coarse resolution ECHAM5-MPIOM atmosphere ocean model simulations were carried out, though with a very low horizontal resolution of T31 (henceforth T31EH5). In such a coupled model, the atmosphere as well as the ocean and the vegetation were simulated and interact with each other and generated its own SST, sea ice and vegetation parameters. This SST anomalies and sea ice cover was then used for an uncoupled ECHAM5 T106 atmospheric simulation (T106EH5).

The models were run on the one hand with the present-day conditions concerning the orography, solar radiation, land ice cover and pre-industrial atmospheric CO_2 concentrations (280 ppm). On the other hand the models were run under LGM conditions concerning these parameters (atmospheric CO_2 concentration – 200 ppm for the ECHAM3 simulation, 185 ppm for the ECHAM5 simulations). In the ECHAM5 runs also CH_4 has changed from 760 to 350 ppb (ctrl to LGM) and N_2O from 270 to 200 ppb. The ECHAM3 simulation was run with SST anomalies and sea ice distributions as reconstructed by CLIMAP (1981). The high-resolution simulations for the present and the LGM with a T106 resolution (corresponding to approx. 1.125° horizontal resolution, henceforth T106EH5) model with 39 vertical levels were carried out with the ECHAM5 atmospheric model (Roeckner et al., 2003). The boundary conditions, e.g. the SST and vegetation parameters, were taken from the coupled ECHAM5-MPIOM atmosphere ocean dynamic vegetation model (Mikolajewicz et al., 2007) simulations, which have been carried out for the present and the LGM with a spectral resolution of T31 (corresponding to approx. 3.75°) and 19 vertical levels. The experimental setup is largely consistent with PMIP2 and some data from these experiments can be found in the PMIP2 data base. For the T106EH5 simulations, these SSTs were corrected for systematic errors of the coupled run by adding the SST differences between observed SSTs and simulated ones for the present. The largest correction appeared over the central northern Atlantic, halfway between New York and Madrid, providing warmer values up to 8 °C due to a too zonally simulated Gulf Stream. Other areas of large SST corrections are within the Benguela Current reaching St. Helena Island and the Kuro-Shio Current. Otherwise the corrections are generally below 3 °C. The same corrections have been applied for the simulations for the present and the LGM. The SSTs are determining the sea-ice cover.

For defining the topography and the land-sea (L-S) mask, the 5 min data sets from PMIP2 (Peltier, 2004) for 0 ka and 21 ka were interpolated linearly to a T106 grid. For deciding on the L-S mask, at the pixel level of 1/12° grid, a grid point was called land if the topography was larger than zero. After that the pixels were averaged to the T106 grid. Large lakes were not found by this method. To solve this, for the experiment with T106EH5 for the present a standard L-S mask used at MPI was used to incorporate or correct the following lakes: Caspian Sea, Aral Sea, Lake Baikal, some smaller lakes in northern Russia, Lake Vänern in Sweden, the Great Lakes and some further lakes in Canada, Lake Chad, Lake Victoria and a widening of the Congo River creating one grid point regarded as a lake. On the other hand, some smaller fjords on the Greenland coast were assumed to be land. Lake Eyre in Australia is, according to the zero-orography criterion, a lake but as it is mostly dry it was assumed to be land. The same criteria have been used for the LGM data set and the resulting L-S mask was compared with the present-day L-S mask just created. For some northern lakes, the glacier mask utilized over-ruled the question of lake or no lake, e.g. for the Great Lakes. For the Black Sea we took the shape as provided by the PMIP2 data using the zero-level criterion. The provided data set did not have a Caspian Sea although large parts of it are deeper than −100 m. A controversial discussion about the size of the Caspian Sea and the Black Sea during the LGM is still going on (Leroy et al., 2007). It is known that there was a Caspian Sea during LGM. However, it is not known whether it was larger (because of a possible diversion of northward flowing rivers to the south due to glaciers along the Arctic coast or of the Amu-Darya), or smaller (because of a possible drier climate) and therefore, for the LGM simulation, we left it as it is now. The same decision was taken for other lakes.

The coupled ECHAM5-MPIOM atmosphere ocean dynamic vegetation model (Mikolajewicz et al., 2007) also provided the vegetation parameters for T106EH5. Along the Arctic coast of western Siberia, the glacier data and the land using the zero-orography criterion left a gap which would create two large lakes into which the Ob and Yenisey Rivers would discharge. The glaciers north of it would prevent drainage into the ocean and larger lakes would evolve, which Grosswald called Pur and Mansi Lakes (Grosswald, 1980). Using the PMIP2 data, the water level of these lakes would need to rise at least 170 m before the water could drain into the ocean. This level is used in this study to define such lakes.

The interpolation of the SST, sea-ice and vegetation parameters from the T31 resolution of the coupled model simulation to T106, needed for forcing the uncoupled run, was done using bilinear interpolation taking into account land-sea differences. Some grid points, however, needed special consideration because of the large difference in resolution which allowed large differences in topographic heights and had a more structured L-S mask in the T106 resolution.

As a criterion for selecting a suitable 25 year period from the 1500 years of simulation with the coupled model, we decided to use a period of lowest SST variability to avoid extremes (years 2906–2930 were chosen for the present and the LGM).

As the three models used here differed in several aspects, also standard Atmospheric Model Intercomparison Project (AMIP – Gates, 1992) type simulation data were taken into account. AMIP was designed to investigate the performance of different atmospheric models which were driven by the same external forcings including monthly mean observed SSTs. At MPI such simulations with the ECHAM5 model using a range of different resolutions are available (Roeckner, 2003; see also Arpe et al., 2004). From this data set the sole impact of resolution on the model performance can be found. It is referred to below as ROECKNER2003. Ramstein et al. (2007) and Jost et al. (2005) discuss the impacts of resolution on the model results and find in one regional model a significant increase of precipitation compared to the driving global model. The impact of resolution in our simulations will be discussed in Sects. 3 and 4.

3 Differences between the simulations

The main parameters for plant growth and their survival are thermal and hydrological conditions. Therefore below the focus will be on near-surface air temperatures and precipitation. For the understanding of the changes and the differences between the models also some dynamical quantities relevant for the climate of Europe are presented and discussed.

3.1 Sea surface and 2 m air temperatures

Figure 1 shows annual mean SST differences between the LGM and the present (NOW) using different estimates. The SST for the T106EH5 simulation is that extracted from the ECHAM5-MPIOM coupled model. In this presentation both should be identical and therefore are marked here as ECHAM5. CLIMAP (1981) is an estimate used in the PMIP1 simulations and GLAMAP (Sarnthein et al., 2003) is a more recent reconstruction. The differences are obvious. CLIMAP provides the coldest LGM temperatures for the North Atlantic, partly enhanced by the sea-ice, and ECHAM5 the warmest. For the remaining oceans ECHAM5 has the coldest temperatures while the other two have even warmer temperatures in places during the LGM than NOW (red colours), which seems unrealistic. Some areas in the summer hemisphere (not shown) appear much warmer during the LGM than NOW. These are areas which were continents during the LGM while they are oceans now, such as along the NE coast of Siberia or the SE coast of Argentina. For the Atlantic more cooling in the Arctic than in the tropics means a stronger north-south SST gradient during the LGM

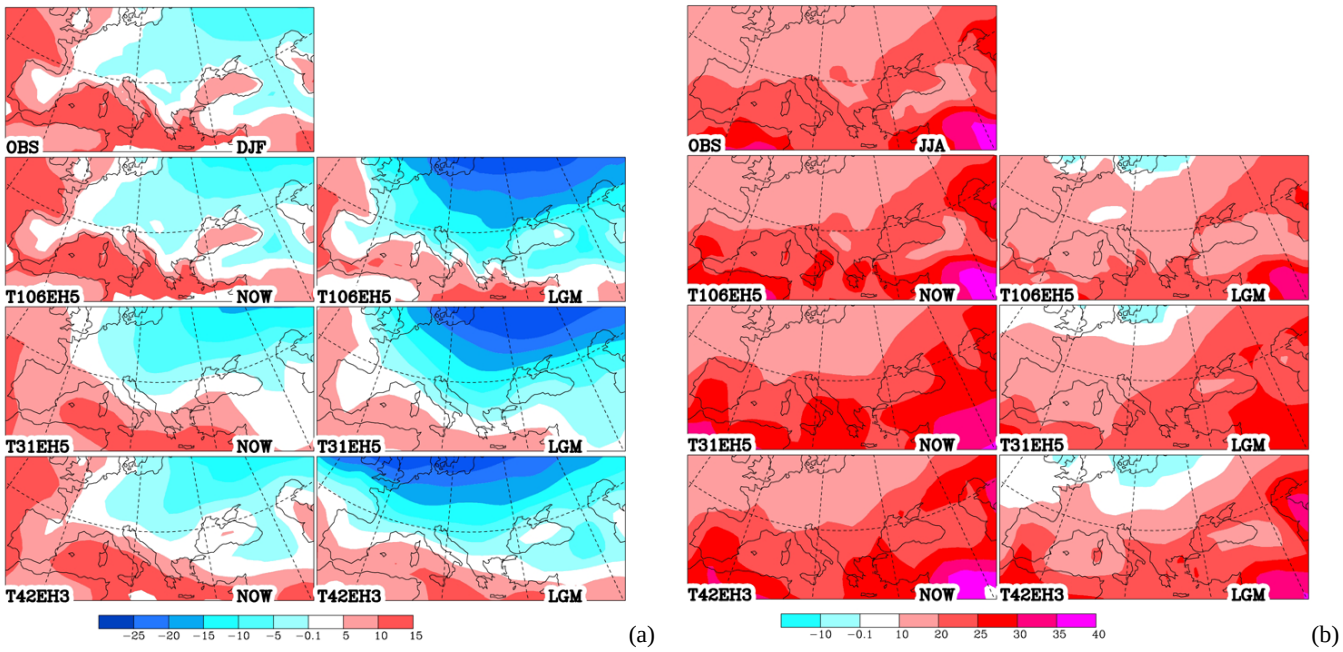

Fig. 2. 2m temperatures for the LGM and NOW as simulated, OBS is the present as analyzed by ERA40 (Uppala et al., 2005), **(a)** for winter, contours every 5 °C, down to −25 °C, **(b)** for summer, contours at −10, −0.1, 10, 20, 25, 30, 35 °C.

than NOW in all simulations, especially in CLIMAP. The CLIMAP simulation for the LGM has much more zonally orientated isotherms and has a very strong gradient over the Atlantic which probably has an impact on the general circulation of the atmosphere (see Sect. 3.2).

The differences in the SSTs and sea ice distributions between CLIMAP and the ECHAM5 simulation are in agreement with PMIP2 (Braconnot et al., 2007). Otto-Bliesner et al. (2009) further suggest that these new simulations are in general agreement with new tropical SSTs reconstructions from the MARGO project (Kucera et al., 2005). The PMIP2 models give a range of tropical (defined as 15° S–15° N) SST cooling of 1.0–2.4 °C, comparable to the MARGO estimate of annual cooling of 1.7 ± 1 °C. This fits well with the ECHAM5 simulations, shown in Fig. 1, which were not included in the PMIP2 runs used by Otto-Bliesner et al. (2009). The PMIP2 models simulate greater SST cooling in the tropical Atlantic than in the tropical Pacific, while the ECHAM5 simulations suggest more cooling for the tropical Pacific.

The consequences of the SST changes for the temperatures over Europe during winter and summer are shown in Fig. 2 where the 2 m temperatures (2 mT), as simulated for the present (NOW) and LGM and as observed using the European Centre for Medium-Range Weather Forecasts (ECMWF) reanalysis data (OBS), are displayed. Comparing the 2 m temperatures of the simulations for the present with the observations shows clearly the best performance of T106EH5, e.g. over western Europe. The differences between the two ECHAM5 simulations are not only due to the different resolutions but also due to differences in the SSTs, as the T106EH5 SSTs are corrected for a systematic error of the coupled model, as explained above. The up to 8 °C cooler SSTs over the North Atlantic in T31EH5 may have led to cooler 2 mT over Europe compared with T106EH5 for the present and LGM. In winter the cooler North Atlantic SSTs with its implications on sea ice during the LGM in the CLIMAP data generate clearly cooler 2 m temperatures for western Europe while the two ECHAM5 simulations provide cooler temperatures for eastern Europe. From ROECKNER2003 one can see that the T106 and T31 simulations would look more similar without the SST corrections in the T106 run.

Note the much more structured cooling over the Alps for summer in T106EH5 during the LGM compared to the other runs shown in Fig. 2b. Here the higher resolution of the model which includes as well a better resolution of the orography shows a direct impact. This turns out to become important in the discussions below. Of further interest for the survival of plants is the temperature variability from year to year. In Table 2 the minimum winter temperature anomalies for three areas in the T106EH5 simulations for the present and the LGM as well as in ERA40 are compared. The increase of anomalies during the LGM by a factor of 2 may be an issue as discussed below.

The T42EH3 run for the LGM provides clearly lower temperatures in summer for most of Europe north of 45° N (the latitude circle in Fig. 2b) compared with the other runs, probably due to the colder North Atlantic SSTs.

Table 2. Extreme cold 2 m temperature anomalies during winter (DJF) in recent years in the ERA40 analyses and in the T106EH5 simulations for the present and for the LGM for land points only on a T106 grid.

	ERA40	T106EH5 NOW	T106EH5 LGM	longitudes	latitudes
Greece	−2.1	−2.0	−5.1	20–25° E	37–41° N
central France	−2.0	−3.7	−8.8	0–5° E	45–50° N
Iberia	−1.7	−2.3	−3.5	10–0° W	36–44° N

3.2 Atmospheric circulation

Figure 3 shows the 500 hPa height fields for the present, overlaid in colour are the differences between the LGM and the present. Blue colours indicate that during the LGM the 500 hPa height field was lower than NOW and red vice versa, e.g. for T106EH5 during winter (Fig. 3 left) the Alaskan ridge and the trough over eastern North America were much stronger during the LGM than for NOW. The T31EH5 model shows similar patterns while the simulation with CLIMAP SSTs and their implications on the sea-ice cover is very different: the ridge over western Europe shown for the present is completely wiped out for the LGM. For summer (Fig. 3 right) the changes from NOW to LGM are less pronounced in all simulations. A slight ridging over eastern Europe during the LGM might be of importance.

In Fig. 4a, the zonal wind for winter (DJF), averaged between 30° W and 10° E (eastern Atlantic and western Europe), is shown in height-latitude cross-sections. The upper panel is the observation as produced by the ECMWF reanalysis (ERA40; Uppala et al., 2005). The lower two panels show the wind as simulated by T106EH5 for the present and the LGM; overlaid in colours are the differences from the field in the panel above, i.e. in the middle panel the colours show the model errors for the present and in the lower panel they show the change between the LGM and the present as simulated by the same model. The T106EH5 simulation for the present has a subtropical jet (20° N, 200 hPa) which is slightly too weak and stretches too far to the south. The polar jet (50° N, 300 hPa) is slightly stronger than observed (ERA40).

During the LGM the polar jet is even stronger and 7° further south while a reduction in the westerlies occurs at 60° N suggesting that the polar jet is forced by the massive ice sheet to go either further south or north of it. This leads to enhanced precipitation over the Mediterranean Sea during the LGM, shown below. The stronger jet fits in as well with the stronger north-south gradient of surface temperatures shown in Fig. 1. Florineth and Schlüchter (2000) suggested from palaeo-data a more southerly position of the main flow during the LGM over the Alps, supporting the simulation by the T106EH5 model.

Synoptic meteorologists who analysed weather maps by hand before the existence of numerical weather forecasts used for winter the −30 °C isotherm at the 500 hPa level as a guide for finding the frontal zone between the polar and mid-latitude air-masses in the middle and upper troposphere. This is dynamically coupled with the jet stream and cyclone tracks. Baese and Arpe (1974) determined these thresholds statistically from radiosonde data for different levels and

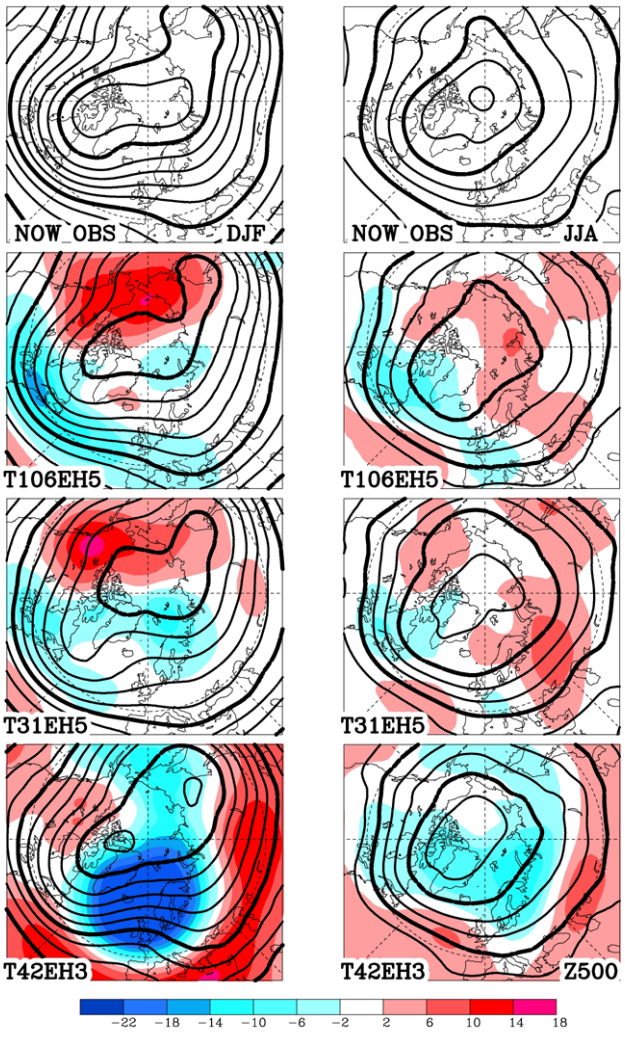

Fig. 3. 500 hPa geopotential height field for the present (heavy lines) overlaid by the difference LGM-NOW (in colours). Contours for the height field every 8 dam (geopotential decametres), highlighted lines for 516 and 556 dam in DJF (left) and for 556 and 580 dam in JJA (right). Contours for the differences at ±2, 6, 10, 14, 18 dam, blue colours for LGM – NOW values < -2, red $> +2$.

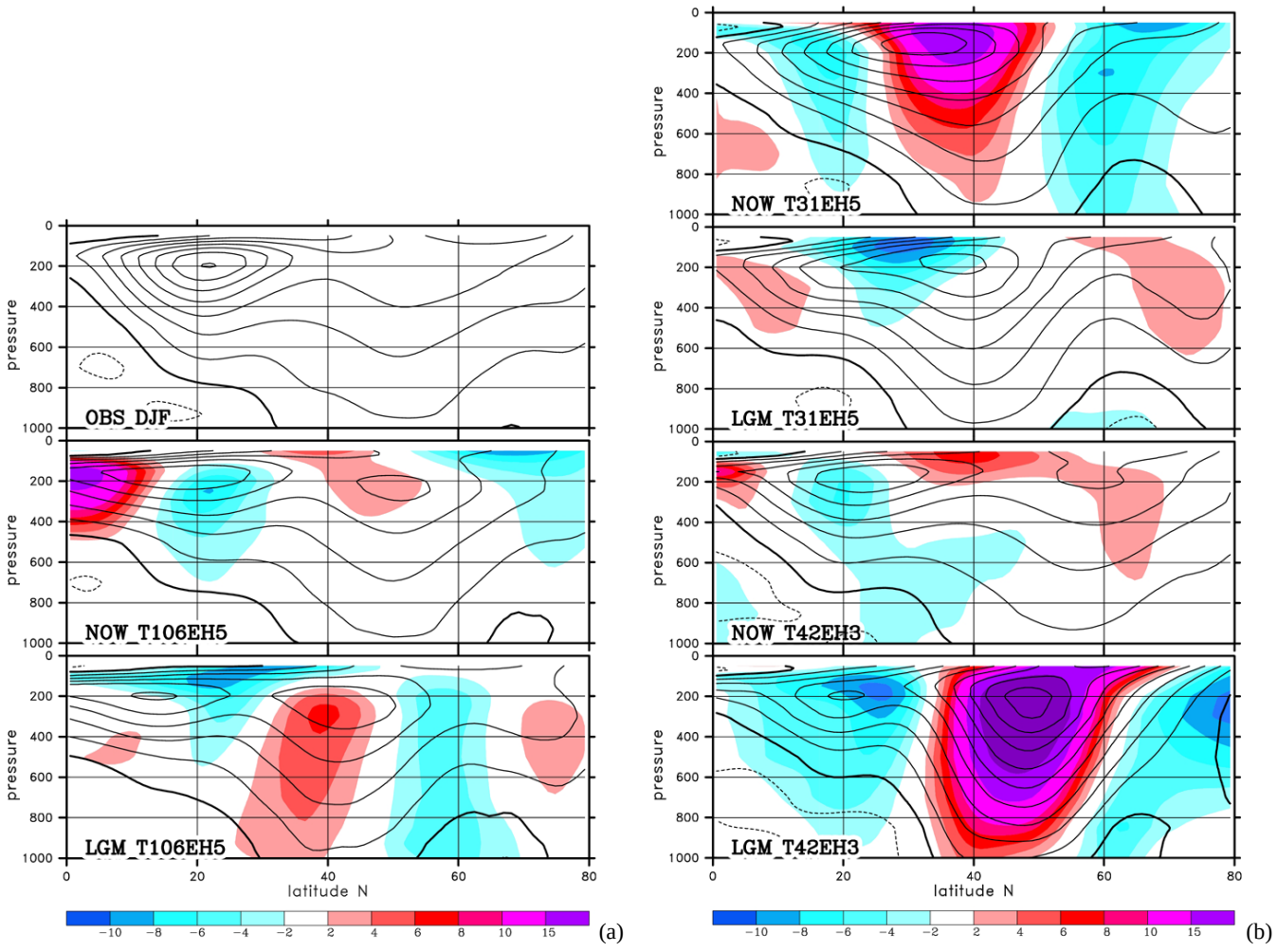

Fig. 4. Latitude-height cross-section of the zonal wind for winter (DJF) averaged between 30° W and 10° E. In the panels for the present (NOW) the differences to the observation are overlaid in colours, i.e. the model error, and in the panels for the LGM simulation the difference to NOW are overlaid in colours. Contours every 5 m s^{-1}, heavy line for the 0-zonal wind contour and dashes for negative values. Red colours for increases by more than 2 m s^{-1} and blue colours for decreases by more than 2 m s^{-1}. **(a)** Analysis (OBS) and T106EH5 simulation. **(b)** T31EH5 and T42EH3 simulation.

seasons. No reason why such fixed thresholds should exist is known. If the same thresholds between air-masses exist also for the LGM one would expect a southward shift of the fronts and jets in a generally colder climate. Here it is shown that the model suggest such shifts for the LGM which means that the threshold between air-masses does not change in a colder climate.

A similar but pole-ward shift of the jet streams and the associated fronts and cyclone tracks has been found for the global warming experiments (e.g. Bengtsson et al., 2006) which can be assumed to be due to the same reason as the equator-wards shift in a colder climate shown here. There have been a lot of speculations about the cause of this shift. Quan et al. (2004) verified model results with observational data for the last 50 years. They draw a connection between the shift of the jet and a widening of the Hadley circulation and found as well an involvement of an ENSO frequency increase. In the T31EH5 simulation in a similar way but with the opposite sign, a decrease of the ENSO frequency was found with an equator-ward shift of the jet for the LGM. However the cause is not fully understood.

Figure 4b shows the same presentation for the T31EH5 and the older T42EH3 simulations. The T31 resolution of T31EH5 is not sufficient for getting the dynamics of the atmosphere completely right and therefore one finds here the largest differences between the simulations for NOW and the observation, indicated by colours in the top panel, presenting the difference between the T31EH5simulation for the present and observations. This model hardly shows a separation between the polar and the subtropical jet. This cannot only be assigned to the difference in the resolution as the ROECKNER2003 data do not show such large differences

with resolution as shown here, which would indicate the influence of the simulated North Atlantic SST error in the coupled model. The difference between the LGM and present-day simulation bears, however, some similarities to those of the T106EH5 simulations. The changes from the present to LGM are strongest in the T42EH3 simulations. The polar jet (50° N, 300 hPa) was already enhanced in T106EH5 for the LGM by more than $2\,m\,s^{-1}$ compared with the present but in the T42EH3 simulation the increase is more than $25\,m\,s^{-1}$, probably due to the much colder SSTs in the northern Atlantic with their implications on the sea-ice cover and warmer tropical SSTs during the LGM in the T42EH3 data compared to the ECHAM5 simulations. Such a stronger north-south SST gradient provides a stronger forcing for the atmospheric circulation. Kageyama et al. (1999), using the same T42EH3 together with other simulations, refer to this enhanced jet stream over the eastern Atlantic as an eastward shift of the jet and found similar shifts in all simulations with the same SST forcing.

LA2007 noticed a massive increase of winter surface wind in the T42EH3 simulations for the LGM over Europe. This can also be seen in the cross-sections of the zonal mean wind at 1000 hPa shown above (Fig. 4b) with increases of $5\,m\,s^{-1}$. In this presentation at this level the differences in wind speed for the other simulations were very small, the differences shown by the colours for T106EH5 mainly mean a southward shift in the position of the maximum wind. Maps of summer and winter mean surface winds (not shown) demonstrate as well a much lesser increase in wind during winter during the LGM for the two ECHAM5 simulations. Common to all simulations is an increase in the Trade Winds off North Africa in summer and an increase in the North Atlantic westerlies in winter for the LGM, which fits well with the enhanced meridional temperature gradient.

3.3 Precipitation

Figure 5a shows the winter (DJF) simulated precipitation for the present (NOW) and the LGM. The estimate by GPCP (Huffmann et al., 1996) using observations is also included. All simulations for the present show similar features to those observed. One can, however, easily see that the T106EH5 simulation fits best to the observations. For the LGM, LA2007 have previously pointed out that the cyclone tracks, indicated by the precipitation patterns, take a very different course in the LGM simulations compared with the present, i.e. during the LGM the cyclones in the T42EH3 simulations move from the British Isles straight eastward into Europe instead of towards Scandinavia as for the present. In T106EH5 a branch towards Scandinavia can still be seen for the present as well for the LGM though weaker for the LGM and a second branch towards the Mediterranean Sea, somewhat stronger during the LGM reaching Lebanon/Israel/Jordan. This branch is clearly further south than in the T42EH3 simulation for the LGM. The T106EH5 simulation with higher precipitation in the Levant is probably realistic as it is known that the Dead Sea had a high stand during the LGM (Stein et al., 2010). The shift of the precipitation towards the Mediterranean Sea during the LGM also fits the study by Florineth and Schlüchter (2000) who found that the precipitation for the Alpine glaciers had their source to the south of them.

During summer (JJA) for the present (NOW), shown in Fig. 5b, the lower resolution model simulations show less precipitation over the northern Atlantic and northern Europe than the observations while T106EH5 is more realistic. Comparing the LGM simulations with those for the present, one finds much less aridity for the LGM in the ECHAM5 simulations (T106 and coupled T31) for Europe than in the T42EH3 simulations, probably due to the much warmer northern Atlantic SSTs in the ECHAM5 simulations. Over western Europe, T106EH5 provides even more precipitation for the LGM compared with the present which has to be assigned to enhanced evaporation over the northern Atlantic during the LGM (not shown).

The differences between the T106EH5 and T31EH5 are not only due to the different resolutions but could also be influenced by the warmer SSTs in T106EH5 as they had been corrected by the systematic error of the coupled run, as described above. From ROECKNER2003 one can find that the T106 and the T31 simulations would look more similar without the SST corrections in T106EH5 but the impacts from resolution alone are dominant. These changes in the precipitation over Europe are consistent with the changes in the upper air wind field as discussed above.

Braconnot et al. (2007) compared the precipitation in the PMIP2 coupled model simulations with the uncoupled PMIP1 simulations and found less drying for central and southern Europe in the PMIP2 coupled simulations, even with an increase of precipitation for western Europe during the LGM in annual means. In annual means for western Europe also the T106EH5 simulation provide an increase in precipitation during the LGM of up to $90\,mm\,season^{-1}$ (not shown) which is similar to the PMIP2 results. The coupled T31EH5 simulations have an increase of only a third of the T106EH5 values. Jost et al. (2005) also find a clear impact of the model resolution on the precipitation. Higher resolution models are able to reproduce the reductions of precipitation found in the palaeo-data more closely than their low-resolution counterparts do; but the simulated climates are still not as arid as reconstructed from palaeo-data. The high-resolution limited area model HadRM even shows increases of annual mean precipitation reaching values similar to those of our high-resolution model. ROECKNER2003 data suggest such an increase of precipitation just from the increased resolution.

It is remarkable that hardly any change occurs between NOW and LGM over the Himalayas both in summer and winter in all simulations, which might be important for the river discharge into the Aral Sea (not shown).

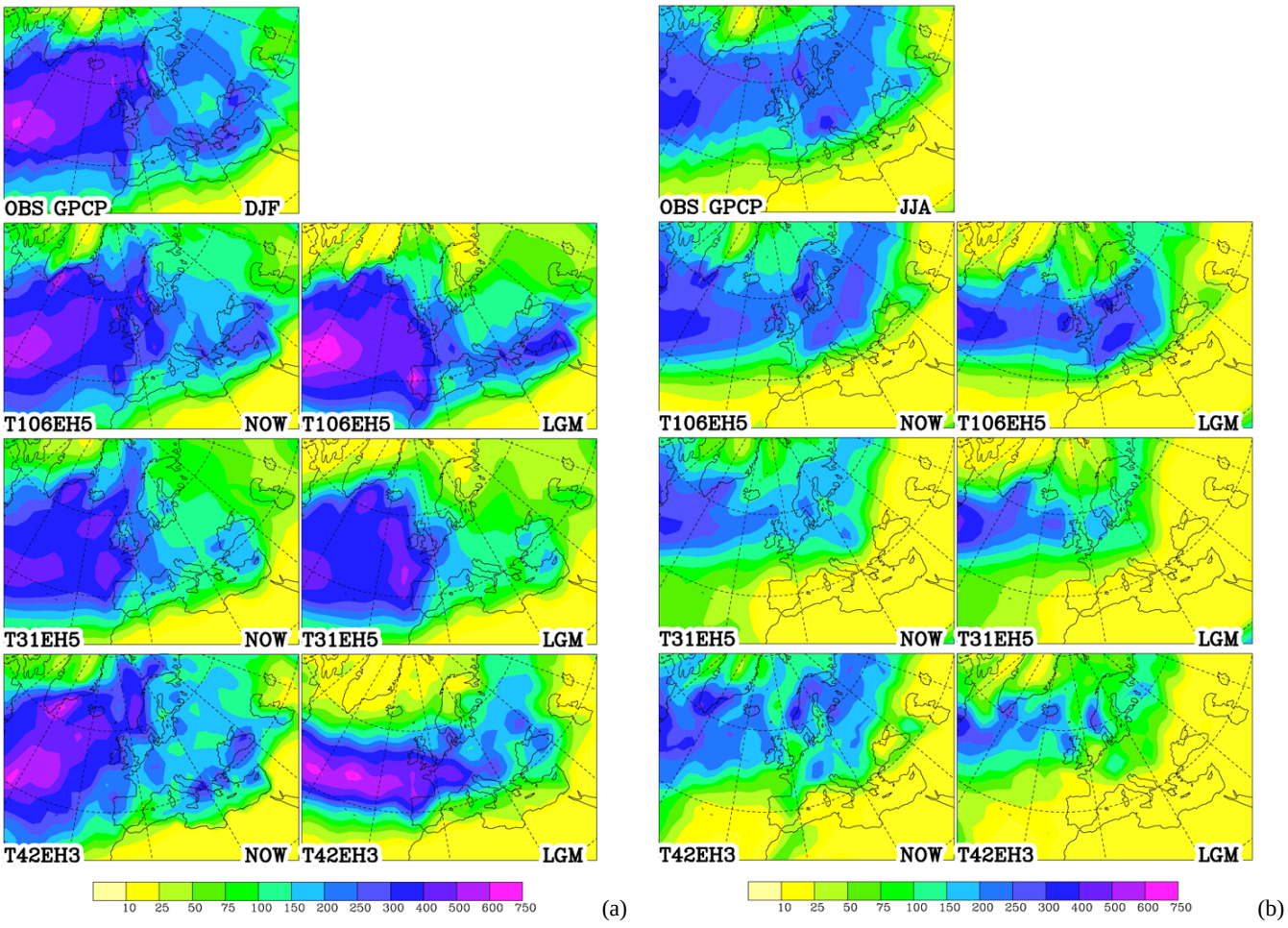

Fig. 5. Precipitation as estimated for the truth (GPCP; Huffman et al., 1996) and simulated by the models. Contours at 10, 25, 50, 75, 100, 150, 200, 250, 300, 400, 500, 600 mm season^{-1}, **(a)** for winter, **(b)** for summer.

3.4 Precipitation minus evaporation

The availability of water for run off and vegetation is best shown by the difference between precipitation and evaporation ($P-E$). In Fig. 6 annual mean differences between LGM and NOW are provided. Because of model constraints, the long-term mean $P-E$ cannot be negative over land as only water which has fallen can be evaporated. For the lower resolution simulations, some negative numbers along coasts can occur over continents due to interpolations to T106, required for the plotting software which results in less strong gradients along coastal lines in Fig. 6. The general reduction of the precipitation shown above for the LGM is not reflected in the $P-E$ plots as the evaporation is also reduced during the LGM. Over western Europe including the Iberian Peninsula $P-E$ is even enhanced in all simulations especially for T106EH5. For Lebanon and Israel in T106EH5 an enhanced availability of water for the LGM is clearly indicated (for T31EH5 only slightly), in accordance with an observed higher stand of the Dead Sea. The ECHAM5 simulations show less water availability during the LGM for eastern Europe. If one is interested in intra- or inter-annual variability the best variable to look at would be the soil moisture but its calculation depends on many less well-known quantities.

Of special concern has been the water budget of the Black, Aral and Caspian Seas. Averages of $P-E$ for the basins of these three seas/lakes suggest that hardly any change occurs between NOW and LGM for the Black Sea, with some decline in the water supply for the Caspian and Aral Seas. For the three lakes/seas the evaporation has similar values for the present as that provided by the ECMWF re-analysis (ERA40; Uppala et al., 2005), while for the LGM the evaporation drops by about a third. The amounts of precipitation drop, however, even more, with the least drop for the Black Sea. These results suggest that the Caspian and Aral Seas should have had a lower level than today and the Black Sea a similar level, unless there has been a diversion of the north-ward flowing rivers due to the blockage by glaciers. The model does not have any constraint concerning the water budget over lakes and seas, while over land the long-term

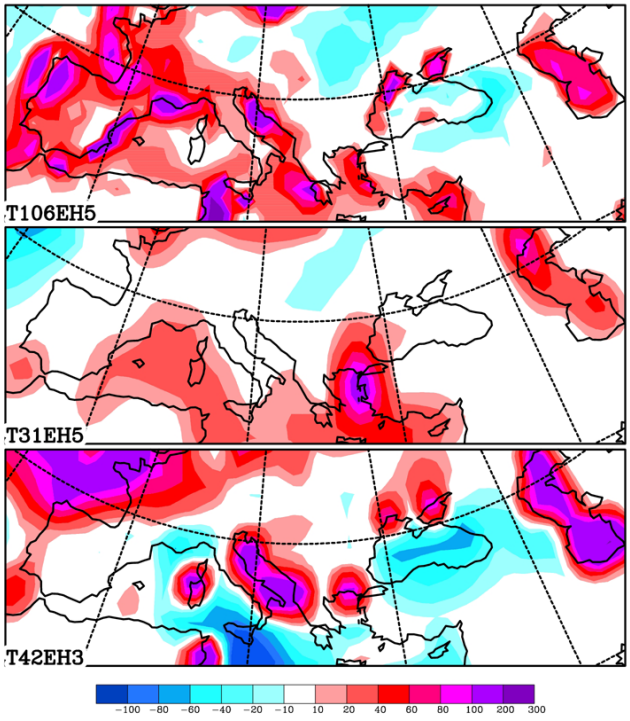

Fig. 6. Annual mean precipitation minus evaporation ($P - E$) in the simulations, difference between LGM and NOW. Contours at ± 0, 10, 20, 40, 60, 80, 100, 200 mm season^{-1}. Negative values are blue, positive red.

mean precipitation has to be larger or equal to the evaporation, therefore no absolute figure can be given.

4 Possible summer-green tree growth during the LGM

So far it has been shown in many examples that the T106EH5 simulation provides the best reproduction of the present climate. Intuitively one may assume that the model which provides best estimates for the present climate would also be best for simulating a climate with a different external forcing such as during the LGM. Validation is, however, difficult; but some aspects have already been discussed above where the T106EH5 simulation seems to be more realistic, e.g. the more southerly position of the cyclone track over the Mediterranean Sea into the Levant, explaining the high stand of the Dead Sea during LGM, and a southward shift of the polar jet. We use here the method from LA2007 to estimate the likeliness of summer-green tree growth during the LGM and compare this with the available pollen, charcoal and fossil wood findings. There, and in this study, a simple down-scaling method is used which partly compensates for systematic errors. For this down-scaling the difference between the simulations for the LGM and for the present is added to a high-resolution climatology of the present (Leemans and Cramer, 1991). The resolution of this climatology

Table 3. Minimum requirements for summer-green tree growth from LA2007 and used in this study.

Parameter	cold-tolerant	warm-loving
mean temperature of coldest month (°C)	−15	−2.5
GDD5 (day °C)	800	1000
summer precipitation (mm season^{-1})	50	60

is 0.5° corresponding to 55 km in meridional and 40 km in longitudinal direction in the area of interest. The following investigation will be done on this resolution although it is known that observational data on their own do not support such a high-resolution and a danger of over-interpretation of the data exists. Still many local features, which might be important for plant habitats especially in mountainous areas are not resolved by this resolution.

A better model should give possible tree growth at more sites with verified growth. Warm-loving and cold-tolerant summer-green trees are investigated. Typical warm-loving trees in this investigation are: *Castanea, Juglans, Platanus, Rhamnus, Fraxinus ornus, Vitis, Quercus pubescens* and *Ostrya*, and cold-tolerant trees are: *Carpinus, Corylus, Fagus, Tilia, Frangula, Acer, Populus, Fraxinus excelsior, Alnus, Quercus robur* and *Ulmus*. More details can be found in LA2007

LA2007 used the summer precipitation, the minimum monthly mean 2 m temperature and the growing degree days (above 5 °C) (GDD5) as limiting factors for possible tree growth. Similarly, for each of these variables and the combined score the possible tree growth in the three simulations is investigated. The minimum requirements for growth of these trees are given in Table 3 which is taken from LA2007.

4.1 Palaeosite selection

A few sites have been suggested as possible refugia for trees during the LGM; but those sites without a proof or where the palaeo-data were not properly dated or did not cover the LGM, were not included in our study. Reliable sites had to have a sub-continuous curve of at least one taxon from our list and an age of 21 ± 2 cal Ka BP.

For a definition of the LGM time we followed the recommendation of EPILOG including the maximum extent of the ice sheet (Mix et al., 2001). Considering the sea-level constraints and the detailed records of regional climatic change available from the ice cores, the EPILOG group reached a consensus that a preferred LGM chronozone can be defined as the interval between 23 000 and 19 000 calibrated years before present (BP), i.e. 19 500–16 100 ^{14}C yr BP. This 4000-yr time window, centred on 21 000 cal yr BP, encompasses the centre of the LGM event defined previously by CLIMAP (1981), and is long enough to allow the inclusion of much existing palaeoclimatic data in a new synthesis. It

is coeval with the lowest stand of sea level (Yokoyama et al., 2000), avoids all known Heinrich Events in the North Atlantic region, and excludes most of Dansgaard-Oeschger climate event 2 (D/O2), as dated in the GISP2 ice core and in the GRIP core with the chronology of Hammer et al. (1997). This definition (21 ± 2 ka) is used here for simulation validation and for deciding if findings of pollen, charcoal or fossil wood from summer-green trees can be assigned to the LGM or not. Peltier and Fairbanks (2006) suggested recently that the time of maximal glaciation started already 3000 years earlier but this was not taken into account in our investigation.

With these requirements of a site to be called reliable, 24 sites have been identified and are listed in Table 4. 13 marine sites fulfil the requirements as well and are also included in Table 4. However, it is often not clear where the pollen found at marine sites came from, either by river or wind transport. Because of the large source area for the pollen, the number of potential grid points needs to be increased. Only little weight was given to these sites for validation.

At the sites 8, 19, 20 and 35, some pollen occurrences of warm-loving trees have been found but do not have the required sub-continuous curve of at least one taxon. Nevertheless we kept them as sites with warm-loving trees, especially those for Greece because they are three nearby sites of the same quality which suggest at least one refugium in the area. For Siles in southern Spain (site 8) the pollen might have been transported from the other nearby sites with warm-loving trees and its inclusion in or absence from our list hardly affects the conclusion of the study.

Most of the sites with identified warm-loving tree reported as well of findings with cold-tolerant trees. In the following all sites with warm-loving trees are assumed to fulfil as well the requirements for cold-tolerant trees to ease the discussion.

Other investigations which compare pollen findings during the LGM with climate model simulations (e.g. Jost et al., 2005) use the spectra in a more complex way, e.g. a regression method. We preferred a more direct approach by which the connections can more easily be seen. In the following we will compare the simulated distributions for precipitation, winter and summer temperature (the latter in the form of growing degree days) with the distribution of cold-tolerant and warm-loving summer green trees and the thresholds associated with the occurrence of these tree types.

4.2 Precipitation

Figure 7 shows the precipitation during the LGM for JJA after a simple downscaling to a 0.5° grid. The much stronger precipitation over western and central Europe in the T106EH5 simulation, especially compared to T42EH3, has already been shown above. Most observation sites (indicated by markers) lie in areas with green or blue colours (meaning more than 50 mm precipitation per season) which are

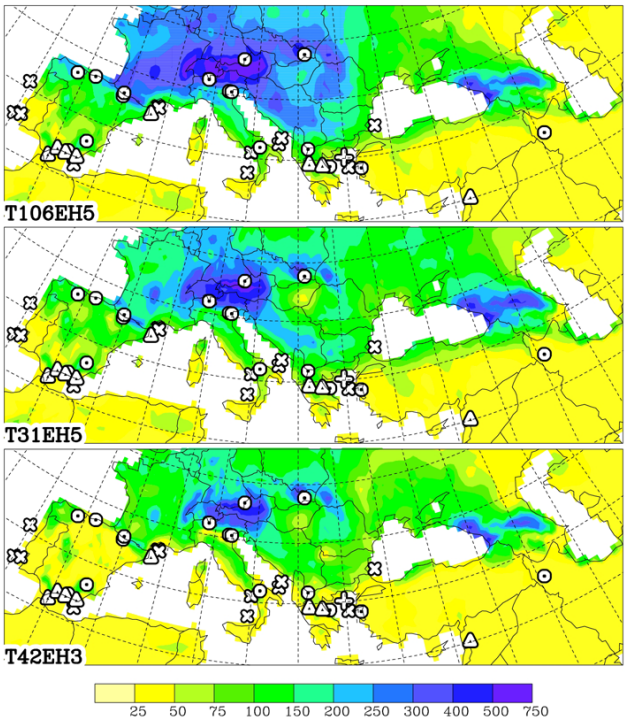

Fig. 7. Summer precipitation during the LGM down-scaled to a 0.5° grid. Contours at 25, 50, 75, 100, 150, 200, 250, 300, 400, 500 mm season^{-1}. Sites with observed summer-green tree growth during the LGM are indicated by markers. Circles: only cold-tolerant trees (continental), triangles: cool or warm-loving trees (continental), Xs: only cold-tolerant trees (marine), crosses: cool or warm-loving trees (marine).

sufficient for possible growth of cold-tolerant trees. Warm-loving trees have a requirement of 60 mm season^{-1} which is hardly different from the 50 mm season^{-1} in the plots. Sites 22, 23 and 24 in Table 4, the easternmost continental sites, lie in areas which have deficient summer precipitation in all three simulations. Sites 23 (Ghab) and 24 (Urmia) are in areas devoid of summer precipitation in the present climate.

A more detailed investigation (see Tables 5 to 7), however, shows that Gibraltar also has too little precipitation when using the nearest grid point, probably because a 0.5° grid is too coarse for capturing the rough topography of this peninsula. One has to look into the surrounding 1.5° away to find a grid point with sufficient precipitation. The T106EH5 simulation provides most precipitation for the grid point covering Gibraltar. The same argument probably applies as well for site 21, a small Greek island along the Turkish coast, though even 1.5° away from the site not enough precipitation can be found; again T106EH5 provides most.

Sites 5 to 7 in southern Spain have too low precipitation in all LGM simulations, highest values in the T106EH5 simulation, which are at the borderline, but one has to look only for neighbouring grid points half a degree away, e.g. in the

Table 4. Reliable continental and marine sites with summer-green tree growth during the LGM from west to east. In column "tree" the letters W mean warm-loving trees and C cold-tolerant trees. The evidence of tree growth comes mostly from pollen analysis, except sites 4 (Altamira) and 5 (Nerja) which have findings of charcoal, and site 2 (Gibraltar) which has evidence from pollen and fossil wood.

No	long	lat	site	seas/ city/country	water depth/ altitude	tree	author
				Group I: reliable continental sites			
1	−6.15	43.05	Lago de Ajo	N Spain	1570	C	Allen et al (1996)
2	−5.30	36.02	Gorham's cave	Gibraltar	0	W + C	Carrión et al. (2008)
3	−4.70	36.80	Bajondillo	S Spain	0–80	W + C	Cortés Sánchez et al. (2008)
4	−4.11	43.38	Altamira	N Spain	70	C	Uzquiano (1992)
5	−3.81	36.75	Nerja	S Spain	158	W	Aura Tortosa et al. (2002)
6	−3.67	37.00	Padul	S Spain	785	C	Pons and Reille (1988)
7	−2.66	36.77	San Rafael	S Spain	0	W + C	Pantaleón-Cano et al. (2003)
8	−2.30	38.24	Siles	S Spain	1320	C some W	Carrión (2002)
9	−0.40	42.73	Tramacastilla	NE Spain	1640	C	González-Sampériz et al. (2005)
10	−0.40	42.99	Formigal	NE Spain	1585	C	IBID
11	3.18	42.04	Laguna Grande	N Spain	1510	W + C	Ruiz Zapata et al. (2002)
12	8.81	46.00	L. di Origlio	Switzerland	416	C	Tinner et al. (1999)
13	11.43	45.29	Po valle	Italy	19	C	Paganelli (1996)
14	11.75	45.27	Lago della Costa	Italy, Po	7	C	Kaltenrieder et al. (2009)
15	12.83	48.16	Duttendorf	Austria	420	C	Starnberger et al. (2009)
16	15.60	40.94	L. Monticchio Neaple	Italy	1326	C	Watts et al. (1996)
17	20.57	48.85	Safarka	NE Slovakia	600	C	Jankovska and Pokorny (2008)
18	20.80	40.90	L. Ohrid	Albania	693	C	Wagner et al. (2009)
19	20.91	39.65	Ioannina	Greece	470	C some W	Tzedakis (1994)
20	22.27	39.50	Xinias	Greece	480	C some W	Bottema (1979)
21	23.05	39.44	Kopais	Greece	95	C	Tzedakis (1999); Okuda et al. (2001)
22	26.30	39.10	Lesvos ML01	Lesbos Greece	323	C	Margari et al. (2009)
23	36.30	35.07	Ghab	NW Syria	240	W + C	Niklewski and Van Zeist (1970)
24	45.33	37.75	Urmia BH2 & BH3	NW Iran	1310	C	Djamali et al. (2008)
				Group II: reliable marine corings			
25	−10.33	40.57	MD95-2039	off Portugal	−3381	C	Roucoux et al. (2005)
26	−10.20	37.77	SU81-18	off Portugal	−3135	C	Turon et al. (2003)
27	−9.51	37.93	SO75-6KL	off Portugal	−1281	C	Boessenkool et al. (2001)
28	−2.62	36.14	MD95-2043	Alboran Sea	−1841	C	Fletcher and Sánchez-Goñi (2008)
29	3.72	42.82	MD99-2349	Gulf of Lions	−126	C	Beaudouin et al. (2007)
30	3.87	42.70	MD99-2348 PRGL1-4	Gulf of Lions	−296	C	Beaudouin et al. (2007)
31	14.49	38.82	KET8003	Tyrrhenian Sea	−1900	C	Rossignol-Strick and Planchais (1989)
32	14.70	40.47	C106	Tyrrhenian Sea	−292	C	Buccheri et al. (2002)
33	17.62	41.29	MD90-917	Adriatic Sea	−1010	C	Combourieu-Nebout et al. (1998)
34	17.91	41.79	IN68-9	Adriatic Sea	−1234	C	Targarona (1997)
35	24.61	40.09	SL152	N Aegean Sea	−978	C some W	Kotthoff et al. (2008)
36	25.00	39.26	MNB3	Aegean Sea	−800	C	Geraga et al. (2010)
37	28.32	42.40	C-2345	W Black Sea	−122	C	Filipova-Marinova (2003)

Sierra Nevada, to find sufficient precipitation and one would hardly call the simulations a failure for these sites. The same applies for sites 19 and 20 in Greece for warm-loving trees. In the T42EH3 run, these sites have extremely low values at the nearest grid point, even sometimes with negative values which can happen due to the down-scaling method when the change from NOW to LGM in the simulations is larger than the observed precipitation at that point.

It has been shown above that the T106EH5 model produced a much wetter western Europe than the other models, even wetter than for the present, and the question is whether that is more or less realistic. The first 11 sites in Table 4 are from Spain and are affected by the precipitation differences. T106EH5 comes closest to reach at least 50 mm season^{-1} for all the sites concerned and gives the best results while T42EH3 the worst. For sites 4 and 7 in southern Spain the

Table 5. Summary of the ECHAM5 T106 run (T106EH5) using JJA precipitation, minimum temperature and growing degree days above 5 °C (GDD5) for continental sites. Values at the nearest grid point of the sites as well as maximum values within a distance ±1 or 3 grid points are given for each variable. Unknown values are marked by * because the climatology assumed this point to be water. The category of trees found during the LGM is given by W for warm-loving trees and C for cold-tolerant trees.

	Distance from site															
	0	±1	±3	0	±1	±3	0	±1	±3	0	±1	±3	0	±1	±3	
no	precip			T_{min}			GDD5			cool score			warm score			obs
1	225	234	234	−0.8	2.5	5.2	953	1653	2655	5	6	6	0	4	6	C
2	36	48	139	6.7	7.4	9.3	2471	2612	3153	0	0	6	0	0	6	WC
3	98	139	139	5.3	7.4	7.4	2202	2612	3526	2	6	6	4	4	6	WC
4	123	172	233	1.3	1.5	2.6	1705	1705	2531	6	6	6	4	4	6	C
5	52	98	175	5.1	5.3	7.4	2290	2289	3526	1	2	6	0	4	6	WC
6	46	132	175	4.3	5.1	7.4	2190	2289	3526	0	4	6	0	2	4	C
7	32	148	175	4.9	6.7	7.6	2419	2899	3526	0	4	6	0	2	4	WC
8	175	175	175	−0.4	2.4	6.7	1031	1678	2899	5	4	6	2	2	4	WC
9	168	364	437	−1.8	3.2	3.8	932	1971	2551	5	4	6	0	4	6	C
10	273	369	437	−3.7	3.2	3.8	509	1971	2551	0	6	6	0	4	6	C
11	144	204	344	4.6	4.6	4.6	2896	2896	2896	6	6	6	6	6	6	WC
12	322	562	580	−7.6	−7.0	−2.4	1404	1591	1621	6	6	6	0	0	2	C
13	188	342	574	−8.9	−6.6	−2.9	1547	1754	1754	7	6	6	0	0	0	C
14	183	334	574	−9.0	−7.9	−2.9	1603	1754	1754	6	6	6	0	0	0	C
15	699	698	698	−15.1	−12.7	−12.0	299	720	943	0	0	4	0	0	0	C
16	121	131	181	−4.0	−0.5	2.9	1140	2024	2591	5	6	6	0	4	6	C
17	393	509	509	−18.2	−15.3	−14.0	657	1246	1536	0	0	6	0	0	0	C
18	120	147	226	−7.0	−4.8	2.1	973	1184	2512	4	4	6	0	0	4	C
19	57	114	131	2.1	2.1	3.6	2432	2432	2924	1	4	5	0	4	4	WC
20	60	88	131	0.1	0.1	3.8	2513	2512	2979	1	2	5	0	4	4	WC
21	63	75	131	−0.3	0.2	3.8	2352	2512	2979	1	2	5	2	2	4	C
22	**	18	47	***	3.2	3.2	****	2946	2946	*	0	0	*	0	0	C
23	5	10	32	5.6	7.6	8.9	3106	3522	3942	0	0	0	0	0	0	WC
24	20	28	83	−6.4	−5.2	2.6	2005	2310	3950	0	0	2	0	0	0	C

difference between the present and the LGM in the T42EH3 simulation was even larger than the observed precipitation leading to negative precipitation values for the T42EH3 run due to the down-scaling method used here. So the wetter Iberian Peninsula in T106EH5 is supported by findings of trees during the LGM.

Also for sites 19–24 the T106EH5 simulation gives highest precipitation though not reaching the 50 mm season^{-1} level. Site 24, Urmia, is a lake in a very arid area in northwestern Iran. Lake Urmia (or Orumiyeh), is one of the largest permanent hyper saline lakes in the world and resembles the Great Salt Lake in the western USA in many aspects of its morphology, chemistry and sediments (Kelts and Shahrabi, 1986). No tree growth can be found in its surrounding area now. Figure 6 suggests only small changes in available water between NOW and LGM, in fact a small decrease in annual mean available water ($P - E$) can be found in the T106EH5 and T42EH3 simulations. Therefore one has to assume that the pollen found there have been transported from further away. The prevailing wind in the ERA40 observation data in May to July, using monthly mean zonal and meridional wind components, is from the east with low wind speeds. This wind is best simulated by the T106EH5 model for the present though with some increase of speed and a slightly more northerly component. The simulation for the LGM hardly differs in this respect from the present. So the source of pollen at Lake Urmia is the coastal area of the Caspian Sea.

Site 23 in Syria is also a very dry area in summer though with sufficient precipitation in spring and winter. Figure 6 suggests some more available water in annual means during the LGM than at the present. At the present time the trees under consideration here could only survive along rivers and it is doubtful that it was much different during the LGM.

Sites 19–21 in Greece are at the borderline concerning precipitation for warm-loving trees in the ECHAM5 simulations, i.e. near 60 mm season^{-1}, while they are much drier in the T42EH3 simulations, providing evidence for

Table 6. Same as Table 5 for the ECHAM5 T31 coupled simulation (T31EH5).

	Distance from site															
	0	±1	±3	0	±1	±3	0	±1	±3	0	±1	±3	0	±1	±3	
no	precip			T_{min}			GDD5			cool score			warm score			obs
1	163	162	162	−2.1	1.5	4.2	454	1013	1905	0	4	6	0	2	4	C
2	32	45	136	5.1	5.9	7.2	1545	1649	2349	0	0	5	0	0	2	WC
3	94	136	136	3.3	5.9	6.8	1285	1649	2276	2	4	5	2	2	2	WC
4	70	117	153	−0.3	−0.1	1.1	967	967	1852	1	3	6	0	0	4	C
5	46	93	167	3.3	3.3	6.8	1303	1302	2276	0	2	5	0	2	2	WC
6	40	125	167	2.5	3.3	6.8	1235	1302	2276	0	1	4	0	0	2	C
7	26	142	167	3.2	5.2	6.8	1404	1826	2276	0	1	3	0	0	2	WC
8	168	167	167	−2.3	0.4	5.2	559	970	1826	0	2	3	0	0	2	WC
9	111	281	355	−2.8	2.1	2.7	541	1389	1721	0	1	6	0	2	4	C
10	190	281	355	−4.6	2.1	2.7	176	1340	1721	0	2	6	0	0	4	C
11	128	178	293	4.8	4.8	5.3	2392	2391	2391	6	6	6	6	6	6	WC
12	244	477	488	−7.0	−6.5	−2.0	1046	1230	1241	5	5	6	0	0	0	C
13	130	274	497	−6.3	−4.7	0.0	1190	1412	1412	5	5	5	0	0	2	C
14	129	270	497	−5.8	−4.8	0.0	1250	1412	1412	5	5	6	0	0	2	C
15	625	625	625	−13.9	−11.8	−10.0	76	389	572	0	0	0	0	0	0	C
16	98	110	152	−4.5	−1.0	1.9	706	1552	1950	0	3	3	0	2	2	C
17	276	402	402	−15.4	−12.4	−10.5	492	1058	1421	0	4	4	0	0	0	C
18	105	121	195	−8.9	−7.1	−0.1	769	988	2140	0	3	6	0	0	0	C
19	47	109	123	−0.1	−0.1	2.9	1912	1912	2341	0	3	4	0	0	0	WC
20	59	87	123	−1.8	−1.8	2.9	2141	2140	2419	1	2	4	0	0	2	WC
21	64	75	123	−2.7	−1.8	2.9	2005	2140	2419	1	2	4	0	2	2	C
22	**	19	47	***	0.4	0.9	****	2593	2593	*	0	0	*	0	0	C
23	4	10	31	3.3	4.8	6.1	2406	2762	3156	0	0	0	0	0	0	WC
24	22	30	95	−6.3	−5.4	1.4	1592	1832	3229	0	0	2	0	0	0	C

the superiority of the more recent model with their changed boundary conditions.

The three marine sites off Portugal are quite distant from land with sufficient precipitation for tree growth. Naughton et al. (2007) nicely showed that modern samples from marine core tops located SW of Lisbon have similar pollen spectra (more Mediterranean type) as found in the upper part of the Tejo/Tajo river in Spain, i.e. the pollen must have travelled down stream for more than 5 degrees which corresponds to 10 grid-points in our investigation. In this upstream area T106EH5 shows enough precipitation to suggest possible tree growth also for the LGM. Naughton et al. (2007) show as well that the more northern site off Portugal have a pollen spectrum similar to the ones in Galicia, again an area which is further than 3° away from the site and which show enough summer precipitation for tree growth in the climate simulations by all three models.

4.3 Temperatures of coldest month

A further limiting factor for summer-green tree growth is the minimum monthly mean temperature. Earlier it has been shown that the T42EH3 simulation is quite different in this respect, cooler in western and warmer in eastern Europe, compared with the two ECHAM5 simulations, probably due to its much colder North Atlantic. This can be seen in Fig. 8, the down-scaled presentation, as well as in Fig. 5b, especially over eastern Europe and Turkey. The T106EH5 simulation shows warmer temperatures for Iberia and NW Africa than the T31EH3 simulations. Again ROECKNER2003 suggests that the difference between the two runs is due to the warmer SSTs in the North Atlantic in the T106EH5 simulation. For most of Iberia one finds observation sites in the white or red areas ($> -2.5\,^{\circ}$C) more so in the T106EH5 simulation, i.e. areas with possible growth of warm-loving trees. The exception is at the grid point of site 10 (Spanish Pyrenees) where also only cold-tolerant trees have been found. The same applies for the T42EH3 simulation at sites 4, 9 and 10. The temperature of the coldest month does not suggest superiority for any of the simulations for western Europe.

Two sites in the Po Valley (sites 12 and 13) fail on this criterion for the warm-loving trees in all simulations, with the worst in the T106EH5 simulation (-9 versus $-5\,^{\circ}$C). Neither site reports the existence of warm-loving trees, however,

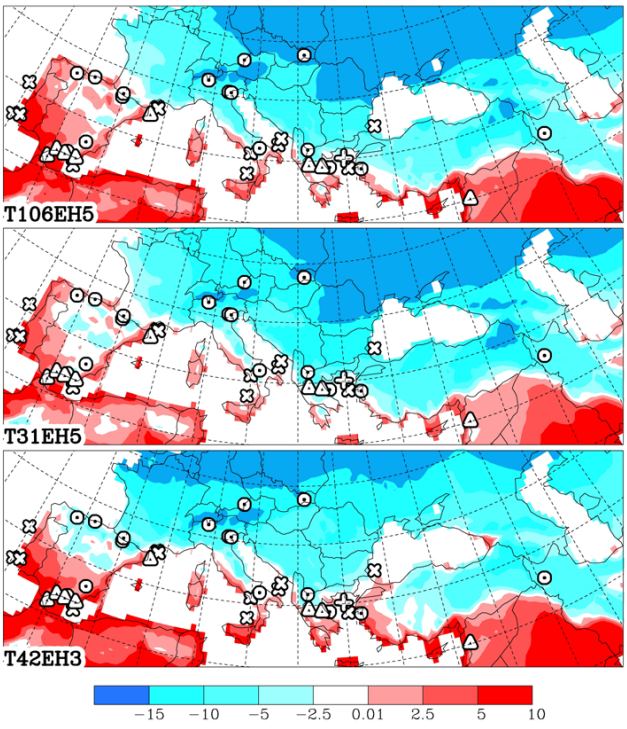

Fig. 8. 2 m temperature of the coldest month. Contours at ±0, 2.5, 5, 10, 15 °C. Sites with observed summer-green tree growth during the LGM are indicated by markers. Circles: only cold-tolerant trees (continental), triangles: cool or warm-loving trees (continental), Xs: only cold-tolerant trees (marine), crosses: cool or warm-loving trees (marine).

a nearby coring in the Venice Lagoon (Canali et al., 2007) shows findings of *Ostrya*, a warm-loving tree, and cores covering the LGM in the Venetian Po Plain show poorly documented occurrences of *Castanea sativa* type (Miola et al., 2006). These sites have not been included in our list of reliable sites because they do not meet our requirements for being categorised as reliable sites. They are mentioned here because these two sites do not agree with the simulated climate. In Fig. 2a it could be seen that the winter temperature difference between NOW and LGM is much more pronounced over and around the Alps in the T106EH5 simulation compared with the others. This can be assigned to the different representation of the Alps and the Adriatic Sea in the different resolutions of the models. LA2007 showed in their Fig. 1 a better representation of the Alps in a T106EH5 model though with a southward shift of the Po Valley, while the other resolutions did not have a Po Valley at all. This and a resolved Adriatic Sea creates a much warmer (more realistic) winter temperature for the present in the T106EH5 simulation than in the lower resolution models. As the downscaling method uses only the difference between LGM and NOW from the simulation, it results in cooler temperatures during the LGM in Fig. 8 for the Po Valley in the T106EH5 simulation.

At the grid points of the two sites 15 and 17 in Austria and Slovakia, only the T106EH5 simulation has values below −15 °C (less cold in the other two simulations), which does not agree with the findings of trees there. The other simulations fail at these stations because of the growing degree days criterion (see below). The largest differences between the models are at site 17 with temperatures of −18.2 (T106EH5) versus −13.5 °C (T42EH3). Perhaps these sites lie in areas with a local climate which is not resolved by the present data and a higher resolution climatology model might alter this finding. Using the Peltier (2004) orographic data on a 5 min grid, one finds a variation between minimum and maximum heights on a 1° grid from 127 to 1308 m; though the mean for a 0.5° grid, the one used here for the climatology (Leemans and Cramer, 1991), has a height of 555 m near to the one at the site of pollen findings during the LGM. A range of heights of 127 to 1318 m corresponds to a temperature range of 8.8 °C when applying a standard atmospheric lapse rate. Also the slope aspect of the terrain to the north or south would be important in such strongly orographically structured area and the trees may have grown on the south facing slopes.

At several sites across Europe, Peyron et al. (1998) estimated the coldest mean temperature and annual mean precipitation by grouping pollen taxa into plant functional types (PFTs). These reflect the vegetation in terms of biomes which have a wider distribution than a species. For the present-day, one can provide a range of minimum temperatures and precipitation in which such PFTs can grow. As the same PFTs can also be found during the LGM, it allows the estimation of ranges of minimum temperatures and precipitation during the LGM. Some of their sites are the same as those used in this study, i.e. sites 6, 16, 19, 20 and 23 (Table 4). At these sites the minimum temperatures given in this study are much warmer than those suggested by Peyron et al. (1998). This suggests for the two Greek sites (19 and 20) that warm-loving trees could not have grown according to the PFT method although some pollen grains have been found there. They also provide annual mean precipitation estimates at these sites which are much lower than those provided by all three model simulations (not shown). More recently Wu et al. (2007) could show that the impact of lower CO_2 on pollen production during the LGM was not taken care of in earlier estimates. Their new estimates of temperature from pollen findings brought a better agreement to the climate based on model simulations of the LGM (Ramstein et al., 2007). Still the new estimates of the temperature of the coldest month in their studies are up to 5 °C cooler than in the present study. They show also the range of uncertainty in their estimate which is larger than 5 °C. As there is not such a discrepancy between palaeo-data and model simulations in the present study we did not follow up this comparison any further.

On the whole it cannot be judged from the available data, whether the large-scale differences in the patterns of the

Table 7. Same as Table 5 for the ECHAM5 T31 coupled simulation (T31EH5).

	Distance from site															
	0	±1	±3	0	±1	±3	0	±1	±3	0	±1	±3	0	±1	±3	
no	precip			T_{min}			GDD5			cool score			warm score			obs
1	112	112	127	−5.6	−1.5	1.8	869	1464	1809	2	3	4	0	2	4	C
2	17	27	124	7.1	8.2	8.9	2899	3165	3858	0	0	6	0	0	6	WC
3	73	120	124	6.1	8.2	9.9	2763	3165	3963	1	6	6	2	6	6	WC
4	−6	38	67	−3.4	−3.1	0.9	1583	1583	2699	0	0	1	0	0	2	C
5	20	72	127	6.3	6.3	9.9	2809	2809	3963	0	1	6	0	2	6	WC
6	9	90	127	5.8	6.3	9.9	2665	2809	3963	0	2	6	0	2	6	C
7	−15	100	127	6.8	8.8	9.9	2900	3309	3963	0	4	5	0	2	4	WC
8	127	127	127	1.2	3.7	8.8	1459	2115	3309	5	5	5	2	2	4	WC
9	18	181	253	−4.0	0.9	0.9	1126	2051	2367	0	0	6	0	0	4	C
10	92	181	253	−7.1	0.4	0.9	686	2051	2367	0	6	6	0	0	4	C
11	90	121	219	4.3	4.3	4.6	2553	2552	2552	2	6	6	4	6	6	WC
12	125	344	367	−7.8	−7.3	−2.3	1517	1695	1782	6	6	6	0	0	2	C
13	46	171	395	−6.6	−4.9	0.2	1758	2045	2045	0	6	6	0	0	4	C
14	48	170	395	−6.3	−5.2	0.2	1827	2045	2087	0	6	6	0	0	4	C
15	543	542	542	−15.3	−12.7	−10.6	97	461	968	0	0	4	0	0	0	C
16	78	89	129	−3.1	0.5	3.6	1303	2269	2822	2	2	4	0	4	4	C
17	275	397	397	−13.5	−10.4	−8.0	157	674	1118	0	0	3	0	0	0	C
18	52	68	122	−6.1	−4.7	2.6	1393	1539	2715	1	1	3	0	0	0	C
19	13	69	74	2.6	2.6	6.2	2569	2568	3010	0	1	1	0	0	2	WC
20	28	62	76	1.1	1.1	6.2	2715	2715	3010	0	1	2	0	2	2	WC
21	34	50	76	0.7	1.1	6.2	2545	2715	3010	0	1	2	0	0	2	C
22	**	5	25	***	5.4	5.7	****	3006	3006	*	0	0	*	0	0	C
23	3	8	29	6.0	8.1	9.6	3226	3626	4019	0	0	0	0	0	0	WC
24	13	22	54	−4.8	−3.6	3.2	2203	2466	4051	0	0	1	0	0	0	C

minimum temperature are more realistic in the one or the other simulation. Also the estimates by Wu et al. (2007) do not help in this respect.

Kageyama et al. (2006) noticed in the PMIP2 model simulations for Europe during the LGM a significantly higher inter-annual variability in coldest-month temperatures compared to the control runs which means that trees could die already at a warmer mean temperature during extreme years. Our simulations also show an increase of variability of the 2 m winter temperature, stronger e.g. for central France than Iberia or Greece. We are not sure about its significance as there would be more snow during the LGM than NOW and more for central France than Iberia or Greece. Such an increase of snow cover results into a much stronger drop of temperature during nights in winter. More relevant for the survival of trees is the temperature within the top few centimeters of the soil and also there the temperature variability is increased during the LGM. In central France the amplitude of January temperature increases from about 3 to 5.5, for Iberia from 1.5 to 3.5 and for Greece from 1 to 2 °C. Absolute winter minima anomalies of single years for the T106EH5 simulations as well as for the ERA40 data are given in Table 2. Above we have required for cold-tolerant tree growth a minimum mean temperature of more than −15 °C. Perhaps one should raise this limit by the increased amplitude of temperature variability.

4.4 Growing degree days

The growing degree days above 5 °C (GDD5) is a less strong limiting factor for tree growth than precipitation. Only a few sites in T106EH5 are in or near areas with values < 800, needed for the growth of cold-tolerant trees, i.e. sites 10 in the Pyrenees, 15 in Austria and 17 in Slovakia of which sites 15 and 17 failed on the minimum temperature (Fig. 9). In the other two simulations, these sites also failed on this criterion. Further sites in T31EH5 (8, 9, 16 and 18) failed at this criterion as well. For most of these sites sufficient GDD5 values are reached only one grid point away from the site, so it might only be a resolution problem. Only Duttendorf in Austria and Safarka in Slovakia (sites 15 and 17) fail on this criterion in the T42EH3 run and only Duttendorf in T106EH5 also for ±0.5°.

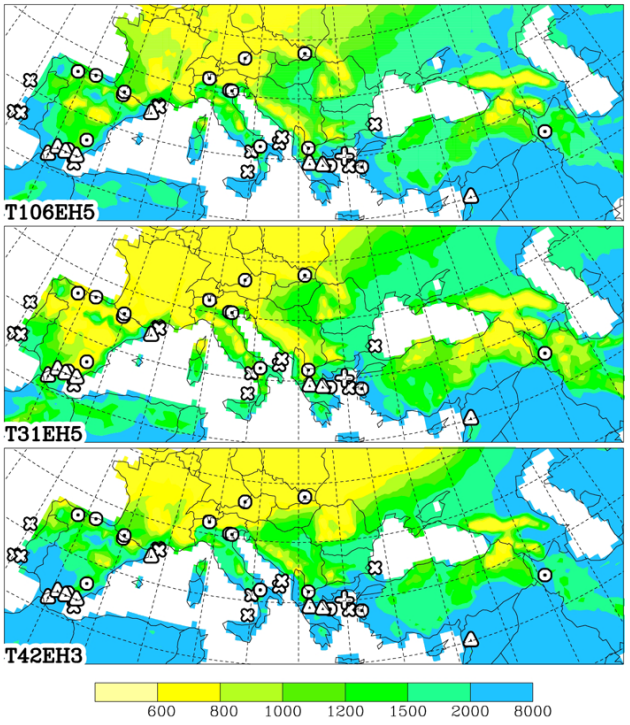

Fig. 9. Growing degree days above 5 °C. Contours at 600, 800, 1000, 1200, 1500, 2000, 8000. Sites with observed tree growth during the LGM are indicated by markers as in Fig. 7.

GDD5 turns out to be a more stringent criterion than the temperature of the coldest month, probably because it represents the growing season while the temperature of the coldest month represents the dormant season and might be responsible for killing the trees when a threshold is passed.

Warm-loving trees need at least 1000 GGD5 which is easily surpassed at all sites with findings of warm-loving trees.

4.5 Summary for summer-green tree growth during the LGM

Possible growth of summer-green trees is found in a belt between too cold temperatures in the north and too low summer precipitation in the south. The topographic impact can clearly be seen as mountains are often connected with enhanced precipitation but also with reduced temperatures. As the limits given by the precipitation are similar for warm and cold-tolerant trees, i.e. 50 mm for cold-tolerant and 60 mm for warm-loving trees, the southern limits for both sorts of trees are very similar. The GDD5 and the minimum temperatures are somewhat complementary but slightly more sites fail on the growing degree days criterion.

In Fig. 10, all limiting factors are taken together. In green or blue coloured areas (values > 1) at least the minimum requirements for all parameters are fulfilled, i.e. for cold-tolerant trees there is more than 50 mm summer precipitation, temperatures of the coldest month are higher than $-15\,^{\circ}$C and the GDD5 values are larger than 800 (60 mm, $-2.5\,^{\circ}$C and 1000 respectively for warm loving trees). Further away from these minimal requirements higher values are given (up to 7) for possible tree growth (darker colours). The T106EH5 simulation produces larger areas of possible tree growth than the other simulations for western Europe while the T42EH3 run suggests more tree growth in eastern Europe, especially north of the Crimea.

Unfortunately no sites with palaeo-data have been found in these areas with larger differences, France and Ukraine. The detailed contributions from the limiting factors have already been discussed above and only for Spain and Greece a clear advantage for the T106EH5 simulation was shown. The visual impression from Fig. 10a also suggests an advantage for the ECHAM5 simulations at Duttendorf in Austria and Safarka in Slovakia, though the detailed numbers do not confirm it for the grid points next to the sites.

In Fig. 10b one can find two interesting shifts for the warm-loving trees at the eastern coast of the Black Sea and the south-western coast of the Caspian Sea with the different simulations. The likeliness of warm-loving summer-green trees moves from the Black to the Caspian Sea from the T42EH3 to the T106EH5 simulation which is due to a shift in the minimum temperature. But the shift is very small.

Tables 5 to 8 provide the detailed values for each site and have already been used in the discussions above. The values in the neighbourhood of the sites in these tables are the maximum values within ± 1 or 3 grid points calculated for each variable separately. This leads for example in Table 6 for T31EH5 at site 7 to the discrepancy that at ± 1 grid point all single variables suggest possible warm-loving tree growth but not the combined score, as the grid point with sufficient precipitation is different to the grid point with warm enough temperatures. For the marine sites in Table 8 only values for ± 3 grid points are given, as these sites were also mostly submerged during the LGM, and pollen must have been transported from further away. The findings by Naughton et al. (2007) suggest even a transport by rivers over distances of 10 grid points for the sites off Portugal. Therefore the marine sites suggest possible tree growth in Galicia and the upper Tejo/Tajo River where especially the T106EH5 simulation show suitable climate conditions.

Table 9 shows statistics of at how many continental sites with observed tree growth the minimum climate conditions for tree growth using simulation data are met. Better scores are clearly obtained for the T106EH5 run for the cold-tolerant trees when looking at the grid point nearest to the site. For warm-loving trees such an advantage can only be seen for the score at ± 1 grid. When extending the search to $\pm 1.5°$ almost all sites are verified with all simulations except the ones at Lesbos and Syria, in both cases failing on the required summer precipitation. For warm-loving trees only one failure for T106EH5 was found, in Syria, because of summer precipitation. The statistic for warm-loving trees

Table 8. Summary of all simulations for marine sites using JJA precipitation, minimum temperature (T_{min}) and growing degree days above 5 °C (GDD5). Only maximum values within a distance ±3 grid points are given for each variable.

site	T106EH5					T31EH5					T42EH3					
				score					score					score		tree
No	prec	T_{min}	GDD5	C	W	prec	T_{min}	GDD5	C	W	prec	T_{min}	GDD5	C	W	obs
25	37	7.8	2420	0	0	30	5.7	1508	0	0	16	5.6	1895	0	0	C
26	41	8.2	2573	0	0	33	6.0	1591	0	0	18	6.7	2077	0	0	C
27	41	8.2	2573	0	0	33	6.0	1591	0	0	20	6.7	2077	0	0	C
28	148	7.8	3526	4	2	142	6.8	2276	1	0	100	9.9	3963	4	2	C
29	344	4.6	2896	6	6	293	5.3	2391	6	6	219	4.6	2552	6	6	C
30	293	4.6	2896	6	6	253	4.8	2391	6	6	187	4.3	2552	6	6	C
31	31	5.1	901	4	4	110	3.8	2074	1	2	89	6.9	3298	2	0	C
32	181	3.1	2378	6	6	152	2.4	1694	3	2	129	4.0	2448	4	4	C
33	238	2.9	2617	6	6	185	1.3	1950	4	4	118	3.4	2822	3	2	C
34	291	2.9	2617	6	6	225	0.8	1950	6	4	151	1.9	2822	4	2	C
35	134	3.7	2964	5	4	132	0.2	2398	5	2	91	4.0	2872	2	2	WC
36	89	3.8	2979	2	4	95	1.2	2419	2	2	76	4.5	2883	2	2	C
37	160	−5.1	2108	6	0	147	−6.3	2121	6	0	84	1.8	2371	2	0	C

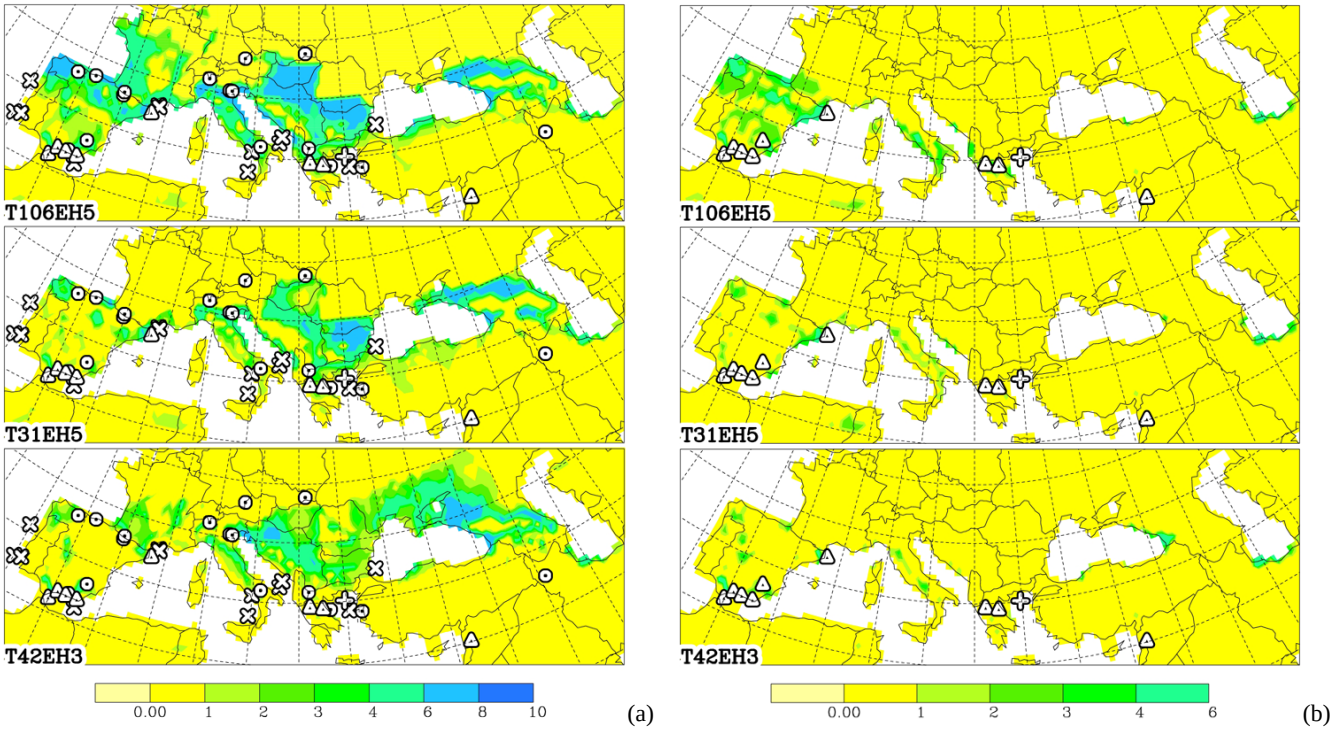

Fig. 10. Possible tree growth during the LGM in the different model simulations combining the summer precipitation, minimum temperature and growing degree days. For values of 1 and higher (green to blue colours) the minimum requirements for possible tree growth are met, higher values mean more summer precipitation and higher GDD5. Sites with observed tree growth during the LGM are indicated by markers as in Fig. 7. **(a)** Cold-tolerant trees, sites with warm-loving trees mostly have evidence of cold-tolerant trees as well. **(b)** Warm-loving trees.

suffers, however, from the uncertainties in the pollen findings at these three sites, as discussed above. All simulations failed to simulate possible tree growth for Urmia in Iran. We assume that the pollen found there has been blown from the coastal area of the Caspian Sea with the prevailing easterly winds in spring and early summer.

It is not clear what the exact minimal required summer precipitation for tree growth is. Laurent et al. (2004) give

Table 9. Number of continental sites with observed tree growth where the simulations suggest possible tree growth at the grid point nearest to the site (0), within ±1 grid point, and within ±3 grid points (±1.5 °) from the site.

cold-tolerant trees									
obs.	T106EH5			T31EH5			T42EH3		
	0	±1	±3	0	±1	±3	0	±1	±3
24	15	18	22	8	19	21	7	16	22
warm-loving trees									
obs.	T106EH5			T31EH5			T42EH3		
	0	±1	±3	0	±1	±3	0	±1	±3
9	3	7	8	2	3	7	3	6	8

a range of tolerance from which one could use also a lower value than the 50 or 60 mm season^{-1} applied here. For cold-tolerant trees at the nearest grid point for T106EH5 from the nine failures, six are due to precipitation. For the warm-loving trees a slight disadvantage exists for T31EH5.

Some genetic studies have postulated formerly unknown refugial areas by pointing to locations with a high genetic diversity, for example Crimea (Comes and Kadereit, 1998). Cordova (2007) and Cordova and Lehmann (2006) suggested that the Crimean coast was a refugium for *Alnus, Carpinus, Corylus, Quercus* and *Ulmus*, i.e. cold-tolerant summer-green trees. Their pollen data did not go as far back as the LGM but, as their earliest data at 12 000 radiocarbon years BP showed pollen from these trees, it is likely that these trees survived the LGM locally. Tsereteli et al. (1982) found pollen of warm-loving and cold-tolerant summer-green trees for the LGM in sufficient numbers to suggest that they were growing locally in Apiancha, Georgia (P. Tarasov, personl communication, 2007). Also their data record did not cover the LGM and therefore both sites are not included in our list of reliable sites; however, both sites are suggested by the model simulations as possible refugia for cold-tolerant trees. Apiancha becomes just too cold for warm-loving trees in the T106EH5 simulation, which is not contradictory to the finding of such trees there as these findings stem from a period before the LGM.

At some sites the simulations suggest the existence of warm-loving trees while the palaeo-data report only cold-tolerant trees. Partly this is due to the fact that some *Quercus* species are warm-loving while others are cold-tolerant and if in doubt we put the palaeo-data in the cold-tolerant category. Furthermore pollen analysis has the deficiency that if one does not find pollen, it does not mean that there were no trees, especially during the LGM since the low CO_2 caused a lower pollen production (Willis et al., 2000; Leroy, 2007; Wu et al., 2007). However, the opposite is valid, though not always valid for the site itself due to possible long-distance transport of the pollen.

Iberia turned out to be an important area for tree refugia because of its higher summer precipitation especially in the T106EH5 simulation compared to the present and still with warm enough winter temperatures. Quite a few sites, also the marine sites off Portugal, with findings of tree pollen or charcoal confirm this model result. This has already been suggested by González-Sampériz et al. (2011) on the basis of palaeo-data.

For down-scaling we have used a method in which the difference between the LGM and present-day simulations are added to a high-resolution present-day climatology. Another method applicable mainly for precipitation is to multiply the ratio of LGM over present-day simulation values with a present-day climatology. This method has the advantage that it will not give any negative values for precipitation. If the simulation of the present-day is perfect, the two methods should give the same result. For the T106EH5 simulations this method gives only slight changes with slightly higher precipitation over Iberia and slightly lower precipitation for parts of eastern Europe. For Iberia it means that all sites in Iberia, including Gibraltar, would have received enough summer precipitation to allow the growth of trees while the values for the other sites hardly differ. The other two simulations are much more affected; they lose possible tree growth for Italy, Greece and the Caucasus area. The T42EH3 run is the most affected with a loss of most areas with possible tree growth. For consistency (using the same method for precipitation and 2 m temperature) and being comparable with LA2007, we did not use this method.

One of the limitations of the approach followed in this paper remains the spatial resolution. Our down-scaling method has reached its limit of possible application as a climatology on a 0.5° grid used here has a resolution which is higher than justified by observational data alone. The future will go for higher resolution models, nested or global as done by Svenning et al. (2008).

The present modelling exercise presents relatively large areas with potential tree growth (Fig. 10). In contrast, pollen analyses and pollen transfer function often refer to the same areas as a steppe landscape. The cause for this discrepancy might be found in a depression in pollen production due to other factors than climate such as low CO_2 (Ziska and Caulfield, 2000) or modified ecosystem water balance (Wu et al., 2007). This would also fit with genetic analyses which propose many micro-refugia, both in the areas proposed by this study (therefore a less steppic landscape than reconstructed by pollen analyses and pollen transfer function) and outside (micro-habitats smaller than our spatial resolution).

5 Conclusions

The first aim of this study was to compare three climate model simulations for the LGM and the second aim was to select the best one to create maps with locations of potential summer-green tree refugia. Firstly the ECHAM3 T42 model forced with SST anomalies provided by CLIMAP (1981), a coupled ECHAM5-MPIOM T31 model, creating its own SSTs, and a ECHAM5 T106 model forced with SST anomalies provided by the coupled model were compared.

The T106EH5 simulation for the present has been found in many respects superior to the other model versions, as might have been expected due to the higher resolution and the most recent model formulations but also due to corrected SSTs. The simulation of the 500 hPa height field in winter for the present gives a much better pattern in the T106EH5 than the T31EH5 simulation while the T42EH3 run is somewhere between the other two simulations, suggesting that in this respect the resolution is more important than other parts of the model formulations. As ROECKNER2003 does not show such large differences as shown in this study, other differences in the simulations, e.g. the SST, were important as well. Also the position of the subtropical jet during winter over western Europe is much better simulated in T106EH5 than in T31EH5, the latter not separating the polar from the subtropical jet. Generally the models simulated too little precipitation for summer and winter, least seriously in T106EH5. For summer the precipitation underestimation in T106EH5 is, however, so weak that the model results can hardly be distinguished from estimates of the truth using observations (GPCP).

For the LGM a main difference to the T42EH3 simulations is the less cold North Atlantic with its implication on the sea-ice cover and colder SSTs elsewhere in the new simulations. Reconstructed SSTs by CLIMAP (1981) and GLAMAP (Sarnthein et al., 2003) show warmer values in places of the tropics and subtropics during the LGM compared with the present, which does not agree with more recent reconstructions. The coupled run shows a cooling everywhere, strongest in the Arctic areas but by far less than in CLIMAP and also less than by GLAMAP, and similar to the PMIP2 investigation (Braconnot et al., 2007). The impact was however less strong over Europe. In winter the two ECHAM5 simulations provide for the LGM over western Europe warmer 2 m temperatures and cooler ones for eastern Europe than the simulation with T42EH3.

For T106EH5 during winter the Alaskan ridge and the trough over eastern North America were both much stronger during the LGM than NOW. T31EH5 shows similar patterns while T42EH3 with CLIMAP SSTs is very different: the ridge over western Europe, shown for the present, is completely wiped out for the LGM. From this missing ridge in the LGM run with T42EH3 one would expect cooler temperatures over Europe in agreement with the model results. For summer the changes from NOW to LGM are less pronounced. A slight ridging over eastern Europe during the LGM might be of importance. The polar jet over the eastern Atlantic and western Europe (30° W–10° E) moves in the T106EH5 simulation from about 50° N for the present to 42° N during the LGM which is probably realistic. In the T42EH3 run it is considerably strengthened at the LGM at the same latitude as for the present-day. Common to all simulations is an increase of wind speed in the Trade Winds in summer and an increase in the North Atlantic westerlies in winter for the LGM.

Large-scale differences have been noted in the simulated temperatures of the coldest month for the LGM between the different runs. It was not possible to determine if this is more realistic in the one or the other simulation because of lack of palaeo-data. The precipitation for Europe during the LGM in winter is characterized by a change in the direction of the main passage of cyclones. In the T42EH3 run, cyclones move in winter from the British Isles straight to the east into central Europe instead of towards the north-east as for the present. In the T106EH5 LGM run, the main cyclone passage is towards the eastern Mediterranean Sea which is probably a realistic feature as the eastern Mediterranean was more humid during the LGM than now. For summer the simulations suggest mostly less precipitation during the LGM than for the present. The T106EH5 run clearly has the highest amount of precipitation, and more precipitation during the LGM than NOW for part of western Europe.

The third aim of this study is a comparison between possible summer-green tree growth from pollen, fossil wood and charcoal analyses and model estimates using summer precipitation, minimum winter temperatures and growing degree days (above 5 °C). More sites with palaeo-data of tree growth during the LGM agree with areas of possible tree growth proposed by the T106EH5 simulation than by the other simulations. This is especially true for Iberia, but less conclusive for the rest of Europe. The clear message especially from the T106EH5 simulation is that warm-loving summer-green trees could have survived mainly in Spain but also in Greece in agreement with findings of pollen or charcoal during the LGM. Southern Italy is also suggested by the models as a possible refugium for warm-loving summer-green trees, but no reliable sites with palaeo-data were available to validate it. The importance of the southern coasts of the Caspian and Black Seas for the survival during the LGM already shown by LA2007 is confirmed also when using the more advanced model T106EH5.

Previous climate simulations of the LGM have suggested less cold and more humid climate than that from reconstruction from pollen findings, (e.g. Svenning et al., 2008). Our model results do agree more or less with those of other models, but we do not find a contradiction with palaeo-data because we use the pollen data directly (significant presence of remains from summer-green trees) without an intermediate reconstruction of temperatures and precipitation from the pollen spectra.

Having gained confidence in the usage of the climate model simulations for identifying possible refugia, it might be useful to extend the investigation to other areas of the world. For such an extension of the work the amount of palaeo-data needs to be significantly increased or made available.

Acknowledgements. We are grateful to many individuals and institutions that provided data and information useful to our study. The help of Monika Esch at MPI for setting up and running the T106EH5 simulation was essential for the success of this study. The reviewers gave valuable information and suggestions for improving the manuscript. The Deutsche Forschungsgemeinschaft funded part of this work in the project MISO within the DFG Priority Programme 1266 (INTERDYNAMIK). The simulations were performed at the "Deutsches Klimarechenzentrum" in Hamburg, Germany. The computing time for the T106 simulations was financed by the German ministry of education and research under contract number 438-BMBF.

The service charges for this open access publication have been covered by the Max Planck Society.

Edited by: M. Claussen

References

Allen, J. R. M., Huntley, B., and Watts, W. A.: The vegetation and climate of northwest Iberia over the last 14 000 yr, J. Quaternary Sci., 11, 125–147, 1996.

Arpe, K., Hagemann, S., and Jacob, D.: The realism of the ECHAM5 models to simulate the hydrological cycle in the Arctic and North European area, Nord. Hydrol., 36, 349–367, 2005.

Aura Tortosa, J. E., Jordá Pardo, J. F., Pérez Ripoll, M., Rodrigo García, M. J., Badal García, E., and Guillem Calatayud, P.: The far south: the Pleistocene-Holocene transition in Nerja Cave (Andalucía, Spain), Quatern. Int., 93–94, 19–30, 2002.

Baese, K. and Arpe, K.: Der Jahresgang der charakteristischen Temperatur der Polarfront in verschiedenen Standardniveaus, Meteorol. Rundsch., 27, 100–109, 1974.

Beaudouin, C., Jouet, G., Suc, J.-P., Berné, S., and Escarguel, G.: Vegetation dynamics in southern France during the last 30 ky BP in the light of marine palynology, Quaternary Sci. Rev., 26(7–8), 1037–1054, 2007.

Bengtsson, L., Hodges, K., and Roeckner, E.: Storm Tracks and Climate Change, J. Climate, 19, 3518–3543, 2006.

Boessenkool, K. P., Brinkhuis, H., Schonfeld, J., and Targarona, J.: North Atlantic sea-surface temperature changes and the climate of western Iberia during the last deglaciation; a marine palynological approach, Global Planet. Change, 30(1), 33–39, 2001.

Bottema, S.: Pollen analytical investigations in Thessaly (Greece), Palaeohistoria, 21, 19–40, 1979.

Braconnot, P., Otto-Bliesner, B., Harrison, S., Joussaume, S., Peterchmitt, J.-Y., Abe-Ouchi, A., Crucifix, M., Driesschaert, E., Fichefet, Th., Hewitt, C. D., Kageyama, M., Kitoh, A., Laîné, A., Loutre, M.-F., Marti, O., Merkel, U., Ramstein, G., Valdes, P., Weber, S. L., Yu, Y., and Zhao, Y.: Results of PMIP2 coupled simulations of the Mid-Holocene and Last Glacial Maximum - Part 1: experiments and large-scale features, Clim. Past, 3, 261–277, doi:10.5194/cp-3-261-2007, 2007.

Buccheri, G., Capretto, G., Di Donato, V., Esposito, P., Ferruzza, G., Pescatore, T., Russo Ermolli, E., Senatore, M. R., Sprovieri, M., Bertoldo, M., Carella, D., and Madonia, G.: A high resolution record of the last deglaciation in the southern Tyrrhenian Sea: environmental and climatic evolution, Mar. Geol., 186, 447–470, 2002.

Canali, G., Capraro, L., Donnici, S., Rizzetto, F., Serandrei-Barbero, R., and Tosi, L.: Vegetational and environmental changes in the eastern Venetian coastal plain (Northern Italy) over the past 80,000 years, Palaeogeogr. Palaeocl., 253(3–4), 300–316, 2007.

Carrión, J. S.: Patterns and process of late Quaternary environmental change in a montane region of south Western Europe, Quaternary Sci. Rev., 21, 2047–2066, 2002.

Carrión, J. S., Finlayson, C., Fernández, S., Finlayson, G., Allué, E., López-Sáez, J. A., López-García, P., Gil-Romera, G., Bailey, G., and González-Sampériz, P.: A coastal reservoir of biodiversity for Upper Pleistocene human populations: palaeoecological investigations in Gorham's Cave (Gibraltar) in the context of the Iberian Peninsula, Quaternary Sci. Rev., 27, 2118–2135, 2008.

Cheddadi, R., Vendramin, G. G., Litt, T., François, L., Kageyama, M., Lorentz, S., Laurent, J.-M., de Beaulieu, J.-L., Sadori, L., Jost, A., and Lunt, D.: Imprints of glacial refugia in the modern genetic diversity of *Pinus sylvestris*, Global Ecol. Biogeogr., 15, 271–282, 2006.

CLIMAP: Seasonal reconstructions of the Earth's surface at the last glacial maximum, Geological Society of America, Map Chart Ser., MC-36, 1981.

Combourieu-Nebout, N., Paterne, M., Turon, J.-L., and Siani, G.: A high-resolution record of the last deglaciation in the central Mediterranean Sea: Palaeovegetation and palaeohydrological evolution, Quaternary Sci. Rev., 17(4), 303–317, 1998.

Comes, H. P. and Kadereit, J. W.: The effect of Quaternary climatic changes on plant distribution and evolution, Trends Plant Sci., 3, 432–438, 1998.

Cordova, C. E.: Holocene mediterranization of the southern Crimean vegetation: Paleoecological records, regional climate change, and possible non-climatic influences, The Black Sea Flood Question: Changes in Coastline, climate and Human Settlement, in: NATO Science Series IV – Earth and Environmental Sciences, edited by: Yanko-Hombach, V., Gilbert, A., Panin, N., and Dolukhanov, P., Springer, Berlin, New York , 319–344, 2007.

Cortés-Sánchez, M., Morales-Muñiz, A., Simón-Vallejo, M. D., Bergadà-Zapata, M., Delgado-Huertas, A., López-García, P., López-Sáez, J. A., Lozano-Francisco, M. C., Riquelme-Cantal, J. A., Roselló-Izquierdo, E., Sánchez-Marco, A., and Vera-Peláez, J. L.: Palaeoenvironmental and cultural dynamics of the coast of Málaga (Andalusia, Spain) during the Upper Pleistocene and early Holocene, Quaternary Sci. Rev., 27(23–24), 2176–2193, 2008.

Djamali, M., de Beaulieu, J.-L., Shah-Hosseini, M., Andrieu-Ponel, V., Ponel, P., Amini, A., Akhani, H., Leroy, S. A. G., Stevens, L., Lahijani, H., and Brewer, S.: A Late Pleistocene long pollen record from Lake Urmia, NW Iran, Quaternary Res., 69, 413–420, 2008.

Filipova-Marinova, M.: Paleoenvironmental changes along the southern Black Sea coast of Bulgaria during the last 29 000 years, Phytologia Balcanica, 9(2), 275–292, 2003.

Fletcher, W. J. and Sánchez-Goñi, M. F.: Orbital- and sub-orbital-scale climate impacts on vegetation of the western Mediterranean basin over the last 48,000 yr, Quaternary Res., 70, 451–464, 2008.

Florineth, D. and Schlüchter, C.: Alpine Evidence for Atmospheric Circulation Patterns in Europe during the Last Glacial Maximum, Quaternary Res., 54, 295–308, 2000.

Gates, W. L.: AMIP: The Atmospheric Model Intercomparison Project, B. Amer. Meteor. Soc., 73, 1962–1970, 1992.

Geraga, M., Ioakim, Chr., Lykousis, V., Tsaila-Monopolis, St., and Mylona, G.: The high-resolution palaeoclimatic and palaeoceanographic history of the last 24,000 years in the central Aegean Sea, Greece, Palaeogeogr. Palaeocl., 287, 101–115, 2010.

González-Sampériz, P., Leroy, S. A. G., Fernández, S., García-Antón, M., Gil-García, M. J., Uzquiano, P., Valero-Garcés, B., and Figueiral I.: Steppes, savannahs, forests and phytodiversity reservoirs during the Pleistocene in the Iberian Peninsula, Rev. Palyn. Palaeobot, 162(3), 427–457, 2010.

González-Sampériz, P., Valero-Garcés, B., Carrión, J., Peña-Monné, J. L., García-Ruiz, J. M., and Martí-Bono, C.: Glacial and Lateglacial vegetation in Northeastern Spain: new data and a review, Quatern. Int., 140–141, 4–20, 2005.

Grosswald, M. G.: Late Weichselian ice sheet of northern Eurasia, Quaternary Res., 13, 1–32, 1980.

Hammer, C. U., Andersen, K. K., Clausen, H. B., Dahl-Jensen, D., Hvidberg, C. S., and Iversen, P.: The stratigraphic dating of the GRIP ice core, Special Report of the Geophysical Department, Niels Bohr Institute for Astronomy, Physics and Geophysics, University of Copenhagen, GRIP-GISP CD-ROM (file gripstrt), Copenhagen, Denmark, 1997.

Huffman, G. J., Adler, R. F., Arkin, P. A., Chang, A., Ferraro, R., Gruber, A., Janowiak, J., Joyce, R. J., McNab, A., Rudolf, B., Schneider, U., and Xie, P.: The Global Precipitation Climatology Project (GPCP) combined precipitation data set, B. Am. Meteor. Soc., 78, 5–20, 1996.

Jankovská, V. and Pokorný, P.: Forest vegetation of the last full-glacial period in the Western Carpathians (Slovakia and Czech Republic), Preslia, 80, 307–324, 2008.

Jost, A., Lunt, D., Kageyama, M., Abe-Ouchi, A., Peyron, O., Valdes, P. J., and Ramstein, G.: High-resolution simulations of the last glacial maximum climate over Europe: a solution to discrepancies with continental palaeoclimatic reconstructions?, Clim. Dynam., 24, 577–590, doi:10.1007/s00382-005-0009-4, 2005.

Kageyama, M., Valdes, P. J., Ramstein, G., Hewitt, C. D., and Wyputta, U.: Northern Hemisphere Storm Tracks in Present Day and Last Glacial Maximum Climate Simulations: A Comparison of the European PMIP Models, J. Climate, 12, 742–760, 1999.

Kageyama, M., Laîné, A., Abe-Ouchi, A., Braconnot, P., Cortijo, E., Crucifix, M., de Vernal, A., Guiot, J., Hewitt, C. D., Kitoh, A., Kucera, M., Marti, O., Ohgaito, R., Otto-Bliesneri, B., Peltierj, W. R., Rosell-Melé, A., Vettorettij, G., Weberl, S. L., and Yu, Y.: MARGO Project Members, 2006, Last Glacial Maximum temperatures over the North Atlantic, Europe and western Siberia: a comparison between PMIP models, MARGO sea-surface temperatures and pollen-based reconstructions, Quaternary Sci. Rev., 25, 2082–2102, 2006.

Kaltenrieder, P., Belis, C. A., Hofstetter, S., Ammann, B., Ravazzi, C., and Tinner, W.: Environmental and climatic conditions at a potential Glacial refugial site of tree species near the Southern Alpine glaciers, New insights from multiproxy sedimentary studies at Lago della Costa (Euganean Hills, Northeastern Italy), Quaternary Sci. Rev., 28, 2647–2662, 2009.

Kelts, K. and Shahrabi, M.: Holocene sedimentalogy of hypersaline Lake Urmia, northwestern Iran, Paleogeogr. Paleocl., 54, 105–130, 1986.

Kotthoff, U., Müller, U. C., Pross, J., Schmiedl, G., Lawson, I. T., van de Schootbrugge, B., and Schulz, H.: Lateglacial and Holocene vegetation dynamics in the Aegean region: an integrated view based on pollen data from marine and terrestrial archives, Holocene, 18, 1019–1032, 2008.

Kucera, M., Weinelt, M., Kiefer, T., Pflaumann, U., Hayes, A., Chen, M. T., Mix, A. C., Barrows, T. T., Cortijo, E., Duprat, J., Juggins, S., and Waelbroeck, C.: Reconstruction of Sea-Surface Temperatures from Assemblages of Planktonic Foraminifera: Multi-Technique Approach Based on Geographically Constrained Calibration Data Sets and Its Application to Glacial Atlantic and Pacific Oceans, Quaternary Sci. Rev., 24, 951–998, 2005.

Laurent, J.-M., Bar-Hen, A., François, L., Ghislain, M., and Cheddadi, R.: Refining vegetation simulation models: From plant functional types to bioclimatic affinity groups of plants, J. Veg. Sci., 15, 739–746, 2004.

Leemans, R. and Cramer, W.: The IIASA database for mean monthly values of temperature, precipitation and cloudiness of a global terrestrial grid, International Institute for Applied Systems Analysis (IIASA), RR-91-18, 1991.

Leroy, S. A. G.: Progress in palynology of the Gelasian-Calabrian Stages in Europe: ten messages, Revue de Micropaléontologie, 50, 293–308, 2007.

Leroy, S. A. G. and Arpe, K.: Glacial refugia for summer-green trees in Europe and S-W Asia as proposed by ECHAM3 time slice atmospheric model simulations, J. Biogeogr., 34, 2115–2128, doi:10.1111/j.1365-2699.2007.01754.x, 2007.

Leroy, S. A. G., Marret, F., Gibert, E., Chalié, F., Reyss, J.-L. and Arpe, K.: River inflow and salinity changes in the Caspian Sea during the last 5500 years, Quaternary Sci. Rev., 26, 3359–3383, 2007.

Lorenz, S., Grieger, B., Helbig, P., and Herterich, K.: Investigating the sensitivity of the Atmospheric Global circulation Model ECHAM3 to paleoclimatic boundary conditions, Geolog. Rundsch., 85, 513–524, 1996.

Lucchi, M. R.: Vegetation dynamics during the Last Interglacial-Glacial cycle in the Arno coastal plain (Tuscany, western Italy): location of a new tree refuge, Quaternary Sci. Rev., 27, 2456–2466, 2008.

Margari, V., Gibbard, P. L., Bryant, C. L., and Tzedakis, P. C.: Character of vegetational and environmental changes in southern Europe during the last glacial period; evidence from Lesvos Island, Greece, Quaternary Sci. Rev., 28, 1317–1339, 2009.

Mikolajewicz, U., Vizcaino, M., Jungclaus, J., and Schurgers, G.: Effect of ice sheet interactions in anthropogenic climate change simulations, Geophys. Res. Lett., 34, L18706, doi:10.1029/2007GL031173, 2007.

Miola, A., Bondesan, A., Corain, L., Favaretto, S., Mozzi, P., Piovan, S., and Sostizzo, I.: Wetlands in the Venetian Po Plain (northeastern Italy) during the Last Glacial Maximum: Interplay between vegetation, hydrology and sedimentary environment, Rev. Palaeobot. Palynol., 141, 53–81, 2006.

Mix, A. C., Bard, E., and Schneider, R.: Environmental processes of the ice age: land, oceans, glaciers (EPILOG), Quaternary Sci. Rev., 20, 627–657, 2001.

Naughton, F., Sanchez Goñi, M. F., Desprat, S., Turon, J.-L., Duprat, J., Malaizé, B., Joli, C., Cortijo, E., Drago, T., AND Freitas, M. C.: Present-day and past (last 25 000 years) marine pollen signal off western Iberia, Mar. Micropaleontol., 62, 91–114, 2007.

Niklewski, J. and Van Zeist, W.: A Late Quaternary pollen diagram from northwestern Syria, Acta Bot. Neerl., 19(5), 737–754, 1970.

Okuda, M., Yasuda, Y., and Setoguchi, T.: Middle to Late Pleistocene vegetation history and climatic changes at Lake Kopais, Southeast Greece, Boreas, 30(1), 73–82, 2001.

Otto-Bliesner, B. L., Schneider, R., Brady, E. C., Kucera, M., Abe-Ouchi, A., Bard, E., Braconnot, P., Crucifix, M., Hewitt, C. D., Kageyama, M., Marti, O., Paul, A., Rosell-Melé, A., Waelbroeck, C., Weber, S. L., Weinelt, M., and Yu, Y.: A comparison of PMIP2 model simulations and the MARGO proxy reconstruction for tropical sea surface temperatures at last glacial maximum, Clim. Dynam., 799–815, 2009.

Paganelli, A.: Evolution of vegetation and climate in the Veneto-Po plain during the late-glacial and the Early Holocene using pollen-stratigraphic data, Il Quaternario, 9(2), 581–590, 1996.

Pantaleón-Cano, J., Yll, E. I., Pérez-Obiol, R., and Roure, J. M.: Palynological evidence for vegetational history in semi-arid areas of the western Mediterranean (Almeria, Spain), Holocene, 13, 109–119, 2003.

Peltier, W. R.: Global glacial isostasy and the surface of the ice-age Earth: the ICE-5G (VM2) model and GRACE, Ann. Rev. Earth Planet. Sci., 32, 111–149, 2004.

Peltier, W. R. and Fairbanks, R. G.: Global glacial ice volume and Last Glacial Maximum duration from an extended Barbados sea level record, Quaternary Sci. Rev., 25, 3322–3337, 2006.

Peyron, O., Guiot, J., Cheddadi, R., Tarasov, P., Reille, M., de Beaulieu, J.-L., Bottema, S., and Andrieu, V.: Climatic Reconstruction in Europe for 18,000 YR B.P. from Pollen Data, Quaternary Res., 49, 183–196, 1998.

Pons, A. and Reille, M.: The Holocene and Upper Pleistocene pollen record from Padul (Granada, Spain): a new study, Palaeogeogr. Palaeocl., 66, 243–263, 1988.

Quan, X.-W., Diaz, H. F., and Hoerling, M. H.: Changes in the Tropical Hadley Cell since 1950, in: The Hadley Circulation: Present, Past, and Future, Advances in Global Change Research, 21, edited by: Diaz, H. F. and Bradley, R. S., Springer, The Netherlands, ISBN 978-1-4020-2943-1, 85–120, doi:10.1007/978-1-4020-2944-8, 2004.

Ramstein, G., Kageyama, M., Guiot, J., Wu, H., Hély, C., Krinner, G., and Brewer, S.: How cold was Europe at the Last Glacial Maximum? A synthesis of the progress achieved since the first PMIP model-data comparison, Clim. Past, 3, 331–339, doi:10.5194/cp-3-331-2007, 2007.

Roeckner, E., Arpe, K., Bengtsson, L., Brinkop, S., Dümenil, L., Esch, M., Kirk, E., Lunkeit, F., Ponater, M., Rockel, B., Sausen, R., Schlese, U., Schubert, S., and Windelband, M.: Simulation of the present-day climate with the ECHAM Model: Impact of model physics and resolution, Max-Planck-Institut für Meteorologie Report, Hamburg, 93, 171 pp., 1992.

Roeckner, E.: ECHAM5_T106L31_AMIP Control Run Monthly Means, World Data Center for Climate, CERA-DB "EH5_T106L31_AMIP_MM" http://cera-www.dkrz.de/WDCC/ui/Compact.jsp?acronym=EH5_T106L31_AMIP_MM, last access: 10 December 2010, and ECHAM5_T31L19_AMIP Control Run Monthly Means, CERA-DB "EH5_T31L19_AMIP_MM" http://cera-www.dkrz.de/WDCC/ui/Compact.jsp?acronym=EH5_T31L19_AMIP_MM, (last access: 10 December 2010), 2003.

Roeckner, E., Bäuml, G., Bonaventura, L., Brokopf, R., Esch, M., Giorgetta, M., Hagemann, S., Kirchner, I., Kornblueh, L., Manzini, E., Rhodin, A., Schlese, U., Schulzweida, U., and Tompkins, A.: The atmospheric general circulation model ECHAM5, Part I: Model description, Max Planck Institute for Meteorology, Hamburg, Report no. 349, 2003.

Rossignol-Strick, M. and Planchais, N.: Climate patterns revealed by pollen and oxygen isotope records of a Tyrrhenian sea core, Nature, 342, 413–416, 1989.

Roucoux, K. H., de Abreu, L., Shackleton, N. J., and Tzedakis, P. C.: The response of NW berian vegetation to North Atlantic climate oscillations during the last 65 kyr, Quaternary Sci. Rev., 24, 1637–1653, 2005.

Ruiz Zapata, M. B., Gil García, M. J., Dorado Valiño, M., Valdeolmillos Rodríguez, A., and Pérez-González, A.: Clima y vegetación durante el Pleistoceno superior y el Holoceno en la Sierra de Neila (Sistema Ibérico Noroccidental), Cuaternario y Geomorfología, 16(10-4), 9–20, 2002.

Sarnthein, M., Gersonde, R., Niebler, S., Pflaumann, U., Spielhagen, R., Thiede, J., Wefer, G., and Weinelt, M.: Overview of Glacial Atlantic Ocean Mapping (GLAMAP 2000), Paleoceanography, 18(2), 1030, 8/1–6, doi:10.1029/2002PA000769, 2003.

Starnberger, R., Terhorst, B., Rähle, W., Peticzka, R., and Haas, J. N.: Palaeoecology of Quaternary periglacial environments during OIS-2 in the forefields of the Salzach Glacier (Upper Austria), Quatern. Int., 198, 51–61, 2009.

Stein, M., Torfstein, A., Gavrieli, I., and Yechieli, Y.: Abrupt aridities and salt deposition in the post-glacial Dead Sea and their North Atlantic connection, Quaternary Sci. Rev., 29(3–4), 567–575, doi:10.1016/j.quascirev.2009.10.015, 2010.

Svenning, J.-C., Normand, S., and Kageyama, M.: Glacial refugia of temperate trees in Europe: insights from species distribution modeling, J. Ecol., 96, 1117–1127, doi:10.1111/j.1365-2745.2008.01422.x, 2008.

Tarasov, P. E., Peyron, O., Guiot, J., Brewer, S., Volkova, V. S., Bezusko, L. G., Dorofeyuk, N. I., Kvavadze, E. V., Osipova, I. M., and Panova, N. K.: Last Glacial Maximum climate of the former Soviet Union and Mongolia reconstructed from pollen and plant macrofossil data, Clim. Dynam., 15, 227–240, 1999.

Targarona, J.: Climatic and Oceanographic Evolution of the Mediterranean Region Over the Last Glacial-Interglacial Transition, A Palynological Approach, LPP Contribution Series, No. 7, Utrecht, The Netherlands, 1997.

Tinner, W., Hubschmid, P., Wehrli, M., Ammann, B., and Conedra, M.: Long-term forest fire ecology and dynamics in southern Switzerland, J. Ecol., 87, 273–289, 1999.

Tsereteli, L. D., Klopotovskaya, N. B., and Kurenkova, E. L.: Mnogosloinaya arheologicheskaya stoyanka Apiancha (Abkhazia), in: Chetvertichnaya sistema Gruzii, Metsniereba, Tbilisi, 198–212, 1982.

Turon, J.-L., Lézine, A.-M., and Denèfle, M.: Land-sea correlations for the last glaciation inferred from a pollen and dinocyst record from the Portuguese margin, Quaternary Res., 59, 88–96, 2003.

Tzedakis, P. C.: Vegetation change through glacial-interglacial cycles; a long pollen sequence perspective, Philos. T. Roy. Soci. Lond. B, 345, 403–432, 1994.

Tzedakis, P. C.: The last climatic cycle at Kopais, central Greece, J. Geol. Soc. Lond., 155, 425–434, 1999.

Uppala, S. M., Kållberg, P. W., Simmons, A. J., Andrae, U., da Costa Bechtold, V., Fiorino, M., Gibson, J. K., Haseler, J., Hernandez, A., Kelly, G. A., Li, X., Onogi, K., Saarinen, S., Sokka, N., Allan, R. P., Andersson, E., Arpe, K., Balmaseda, M. A., Beljaars, A. C. M., van de Berg, L., Bidlot, J., Bormann, N., Caires, S., Chevallier, F., Dethof, A., Dragosavac, M., Fisher, M., Fuentes, M., Hagemann, S., Hólm, E., Hoskins, B. J., Isaksen, L., Janssen, P. A. E. M., Jenne, R., McNally, A. P., Mahfouf, J.-F., Morcrette, J.-J., Rayner, N. A., Saunders, R. W., Simon, P., Sterl, A., Trenberth, K. E., Untch, A., Vasiljevic, D., Viterbo, P., and Woollen, J.: The ERA-40 re-analysis, Q. J. Roy. Meteor. Soc., 131, 2961–3012, doi:10.1256/qj.04.176, 2005.

Uzquiano, P.: L'Homme et le bois au Paléolithique en région Cantabrique, Espagne, Exemples d'Altamira et d'El Buxu, Bulletin de la Société Botanique de France, 139, 361–372, 1992.

Wagner, B., Lotter, A. F., Nowaczyk, N., Reed, J. M., Schwalb, A., Sulpizio, R., Valsecchi, V., Wessels, M., and Zanchetta G.: A 40,000-year record of environmental change from ancient Lake Ohrid (Albania and Macedonia), J. Paleolimnol., 41, 407–430, 2009.

Watts, W. A., Allen, J. R. M., Huntley, B., and Fritz, S. C.: Vegetation history and climate of the last 15,000 years at Lagho di Monticchio, southern Italy, Quaternary Sci. Rev., 15, 113–132, 1996.

Willis, K. J., Rudner, E., and Sümeg, P.: The Full-Glacial Forests of Central and Southeastern Europe, Quaternary Res., 53, 203–213, 2000.

Wu, H., Guiot, J., Brewer, S., and Guo, Z.: Climatic changes in Eurasia and Africa at the Last Glacial Maximum and mid-Holocene: reconstruction from pollen data using inverse vegetation modelling, Clim. Dynam., 29, 211–229, 2007.

Yokoyama, Y., Lambeck, K., de Dekhar, P., Johnston, P., and Fifield, L. K.: Timing of last glacial maximum from observed sea level minima, Nature, 406, 713–716, 2000.

Ziska, L. H. and Caulfield, F. A.: Rising CO_2 and pollen production of common ragweed (*Ambrosia artemisiifolia*), a known allergy-inducing species: implications for public health, Aust. J. Plant Physiol., 27, 893–898, 2000.